Climate Change in the Tillamook Bay Watershed

The Oregon Climate Change Research Institute (OCCRI)
Darrin Sharp, Kathie Dello, David Rupp, Philip Mote, Rachel Calmer
May 2013

OCCRI

PROTECTING AND RESTORING 25 YEARS NATIONAL ESTUARY PROGRAM

Tillamook Estuaries Partnership

Executive Summary

The five river basins in the Tillamook Bay Watershed drain from Oregon's northern Coast Range into Tillamook Bay, a shallow estuary that is an important nursery for Oregon fisheries, including the $45 million Dungeness crab industry. This report describes the past climate of the watershed, projects future climate change over the next century and suggests possible impacts. While the scope of this project did not include next steps, it is expected that future reports will identify actions that may provide resiliency against anticipated impacts.

The report focuses primarily on three climate variables — temperature, precipitation and sea level — for which abundant data exist. It also touches briefly on wave height and storminess, snowfall, and ocean acidification.

The Past Century

The following temperature and precipitation trends reflect averages across the Tillamook Bay Watershed, whose climate varies widely from the Pacific Ocean to the Coast Range.

Temperature. The northwestern coast of Oregon is already experiencing climate change in the form of increasing average, maximum, and minimum temperatures. Overall, the Tillamook Bay Watershed has warmed during the last century. Data collected at three climate-quality weather stations in the region show that average temperatures have risen about 1.0 °F in the last 110 years.

Precipitation. Precipitation has remained relatively constant, averaging about 90 inches per year at the Tillamook climate monitoring station. Extreme precipitation events (events in the 99th or 99.7th percentile) have increased slightly, between 0.05 and 0.1 per decade.

Sea Level. In contrast to other coastal regions around the planet, sea levels have dropped in the Tillamook Bay Watershed by about 1.2 inches (31 mm) in the 20th century. This drop in sea level is in contrast to a 6.7-inch (170 mm) rise globally over the same period. Geologic activity off the coast of Tillamook is pushing the coastline upward, accounting for the drop in sea level relative to other regions of the world. However, the change in sea level is mixed across the watershed. Measurements at some points in the region show a rising relative sea level (albeit at less than the global rate). While positive vertical land motion somewhat minimizes the effect of global sea level rise along the Oregon coast, it does not completely neutralize it.

Looking Ahead: Warmer and Wetter

Computerized models were used to project possible future scenarios. To address uncertainty in future greenhouse gas emissions, the report looked at both "low" and "high" emissions scenarios. A "low" emissions model for 2100 estimates atmospheric CO_2 concentrations about 50% higher than today. A "high" emissions model estimates a concentration about 200% higher than today. Both models showed that the region's annual mean temperature will continue to increase. The level of that increase will depend on the quantities of greenhouse gases emitted worldwide.

For projecting into the future, this report looked at two distinct domains within the watershed. The "West" domain runs inland from the coastline to just beyond the city of Tillamook. The "East" domain runs from just beyond the city of Tillamook to the watershed's eastern edge along the Coast Range, which is the watershed's major topographic feature.

Temperature. Given these uncertainties, the Tillamook Bay Watershed is projected to be warmer by between 4 °F and 7 °F by century's end. In the East domain of the watershed, many more days over 90 °F are projected, and the hottest day of the year is projected to be warmer than today's hottest day by as much as 8–9 °F, again depending

on global greenhouse gas (GHG) emissions levels. There also will be significantly fewer days that drop below freezing, according to the model projections.

Precipitation. Annual mean precipitation is projected to increase about 3–5% by 2100 for both domains. Although the fall and winter seasons will be wetter under both scenarios, spring and summer will be drier. Summer precipitation is projected to decrease between 14% and 19%. Spring precipitation will go down by about 3–4% according to the models.

Days getting at least 2 inches of precipitation are projected to increase in number by the end of the century. Both domains are projected to see an increase of 1–3 days per year, depending on global emissions levels.

The wettest day of the year is projected to be even wetter by 2100; both domains are projected to see an increase in precipitation on the wettest day of the year of between 0.25 and 0.75 inches. Note that for all the precipitation extremes, high emissions are associated with more precipitation than low emissions.

The number of drought months (in which precipitation is less than 80% of the historical average) is projected to increase slightly for both domains. Historically, both domains had about 150 drought months per 30-year period. In the future this is projected to increase to about 155–160 drought months per 30-year period.

Sea Level. By 2100, local relative sea level rise is projected to be about 24 inches, with a possible range of 16 to 55 inches. For comparison, global projections are about 32 inches, with a range of 20–55 inches. Vertical land motion (upward lift of the land due to plate tectonics) reduces apparent sea level rise along most of the Oregon coast.

Potential Impacts

This report is necessarily limited in scope to examination of these climate variables. Significant additional research would be required in order to adequately address how changes in these parameters would impact surface hydrology, species richness and/or range, landscape changes, or any number of other impacts.

However, based on existing science, some impacts can be projected.

- Due to warmer and drier summers, wildfire may become more likely.
- The frequency and magnitude of coastal flooding will likely continue to increase, potentially leading to increased property and infrastructure damage.
- Due to sea level rise and inundation, estuarine water quality may decrease.
- Many plant and animal species on land, in freshwater, and in the ocean will likely shift their distributions and become more, or less, abundant. Coastal areas will likely see mixed evergreen and subtropical mixed forests displacing the current maritime evergreen forests. Plant and animal species on land may shift northward and/or upward to find a suitable climate; marine/aquatic species may go deeper. These migrations may include agricultural species.
- While there is still much work to be done in order to develop a complete assessment, the work to date suggests that changes in the climate pose economic risks to the state.

Special Acknowledgements to the Environmental Protection Agency (Climate Ready Estuaries program); the Oregon Climate Change Research Institute; and the Tillamook Estuaries Partnership in making this document possible.

Introduction

Up until this point, no formal work in the area of climate change has focused specifically on the Tillamook Bay Watershed (TBW). After receiving funding through the EPA's Climate Ready Estuaries program, the Tillamook Estuaries Partnership (TEP) collaborated with the Oregon Climate Change Research Institute (OCCRI) in order to conduct an assessment of the potential impacts of climate change on the TBW. This report is the product of this collaboration. It introduces the basic concepts of climate change, assesses potential impacts on the TBW, and provides a foundation for future research efforts.

Over the last 200 years (roughly since the beginning of the Industrial Revolution in the late 18th century), human activities have been changing the composition of the atmosphere, as well as the surface of the earth. For the past several decades, researchers have been evaluating how these changes affect the earth's climate. Well-established science now says that these changes will affect the climate in a variety of ways (IPCC 2007).

These changes in global climate may have important effects on localities such as the Tillamook Bay Watershed. In order to plan for, and perhaps adapt to, these effects it is important to understand the type and magnitude of these changes. This report attempts to outline plausible changes in the Tillamook Bay Watershed so that appropriate management decisions may be considered.

This report describes changes in important and well-measured environmental variables: temperature and precipitation (both means and extremes), and sea level. Both the historical record and possible future climates will be examined. Historical data will be drawn from a variety of sources; future projections will be based on a suite of recent climate models. Other climate related parameters such as wave height, storminess, snow, and ocean acidification are also examined.

The intended audience for this report is anyone who has an interest (whether commercial, environmental, or personal) in the Tillamook Bay Watershed. No specialized training or education in climatology is assumed.

By necessity, the scope of this report must be limited to the examination of select climate and climate-related parameters (e.g., sea level rise). Significant additional research would be required in order to quantify the impacts that a change in temperature, for instance, might have on fishery productivity, surface hydrology, or any other of a number of "downstream" variables.

Description of the Tillamook Bay Watershed

The TBW is located in northwestern coastal Oregon (see Figure 1). The bay itself is a small (13 mi^2), shallow (average depth of 6.6 ft) estuary about 60 mi west of Portland. At low tide, about 50% of the estuary bottom is exposed. The TBW includes five river basins: the Miami, Kilchis, Wilson, Trask, and Tillamook, all of which drain from the Coast Range into Tillamook Bay. The watershed's total area is about 560 mi^2 (Tillamook Summary 1998). The watershed's largest city, Tillamook, has a population of about 5,000.

Commercial uses of the TBW include agriculture, fishing (including shellfish production), and forestry. Land use varies within the watershed, with agriculture primarily on privately owned land in the lower watershed, and forestry primarily occupying publicly owned land in the upper watershed. The valley of the Tillamook River south of Tillamook Bay is home to the dairy farms that make up the cooperative of the Tillamook County Creamery Association (Tillamook Summary 1998).

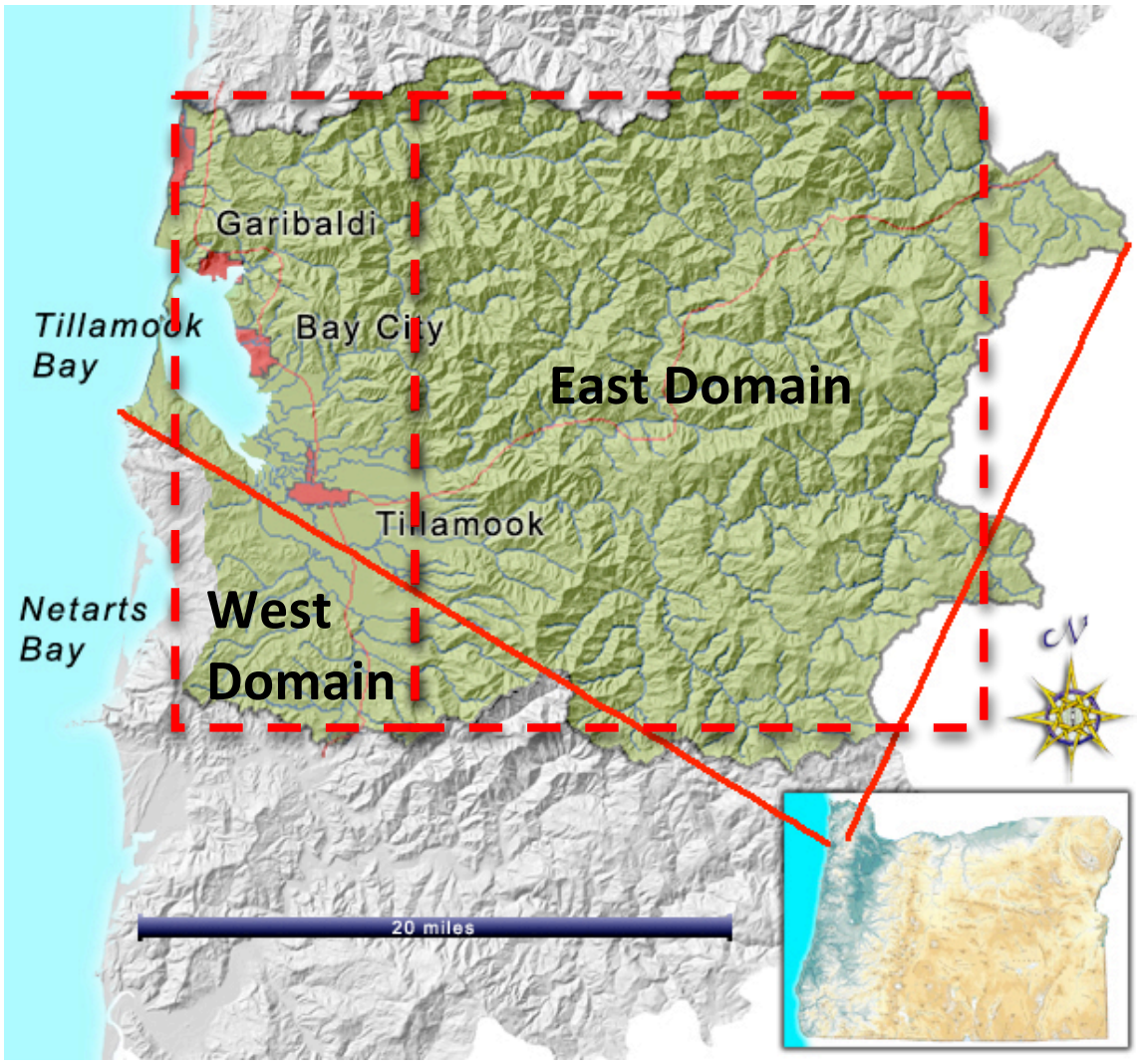

Figure 1: The Tillamook Bay Watershed, showing the East and West domains.

For the purposes of this report, the overall TBW has been divided into an East domain and a West domain (see Figure 1). This division was implemented due to the variation in climate across the watershed (especially along the east–west gradient). If the entire watershed were treated as one domain, important spatial variations would be "averaged out." For example, it is typically much cooler in the summer on the coast than even a short distance inland. By averaging summer temperatures over the entire watershed, this variation would be lost. The east–west dividing line was chosen so as to capture the effect of climate on the Coast Range, and also to allow for computational efficiency during the analysis.

The West domain is defined as 236.05E to 236.20E longitude, while the East domain is 236.20E to 236.55E. Both domains are 45.35N to 45.65N latitude.

Climate Primer

Climate Primer at a Glance

Since the Industrial Age began in the mid-1700s, humans have been using oil, natural gas and coal to heat their homes, run their cars and power their factories. Burning these "fossil fuels"— the remains of ancient life forms that have been buried for eons — gives off carbon dioxide (CO_2), an invisible gas that builds up in the atmosphere. As CO_2 wraps around the planet, it traps and holds heat from the sun, like a greenhouse does. Scientists analyzing ancient layers of ice from places like Antarctica have found that today's global concentration of greenhouse gases is higher than at any time in at least 800,000 years.

As the earth gets warmer, regions around the world are experiencing changes in growing seasons, water quality and abundance, ocean chemistry, coastal erosion, sea level, and wildlife habitat. Ocean chemistry is of particular concern to coastal communities. The oceans absorb CO_2 from the atmosphere. The oceans are vast and, under normal conditions, can safely take up carbon without harming sea life. But when the level of carbon reaches a critical concentration, it tips ocean chemistry, making the seas more acidic. The excess acid interferes with the calcium shellfish need to build their shells. Since the beginning of the Industrial Revolution, the oceans have absorbed something like 127 billion metric tons of carbon (as CO_2) from the atmosphere. This represents about one-third of all human-generated carbon emissions of the last 250 years, scientists estimate. Regions of the west coast, including Oregon, are particularly susceptible to ocean acidification.

Sea level rise, too, is a concern for coastal communities globally. As seawater gets warmer, it expands. Also, as mountain glaciers and polar ice sheets melt, the melted water flows into the oceans, raising sea levels further. Another cause of rising seas is withdrawal of water from reservoirs, such as aquifers, which eventually ends up in the ocean.

Introduction to Climate Change

The amount of energy Earth receives from the sun is only enough to keep its average surface temperature at about 0 °F. The earth is kept at a livable temperature by the heat-trapping effect of greenhouse gases (GHGs). A number of gases contribute to the greenhouse effect; chief among them are carbon dioxide (CO_2), methane (CH_4), and nitrous oxide (N_2O). Of these, CO_2 makes the largest contribution due in part to its residence time in the atmosphere (an average CO_2 molecule remains in the atmosphere, warming the surface, for decades) and its relative abundance (Forster et al. 2007; Kiehl and Trenberth 1997). The atmospheric concentration of CO_2 in the atmosphere has risen from 280 to almost 400 parts per million (ppm) in the past ~120 years. The source of this additional atmospheric CO_2 is human activity, such as fossil fuel combustion (IPCC 2007).

Water vapor, the most powerful greenhouse gas (Kiehl and Trenberth 1997), differs in important ways from CO_2 and other greenhouse gases. First, its lifetime is quite short—a week or so. Second, unlike CO_2 and other greenhouse gases, the concentration of water vapor in the atmosphere is largely controlled by the surface temperature, especially of the ocean and other large water bodies. The concentration of water vapor increases as the temperature increases, and decreases when the temperature decreases. As a result, as the atmosphere warms (as a result of more greenhouse gases, like CO_2), the concentration of water vapor also increases (Santer 1997). In effect, water vapor is part of a positive feedback loop. Water vapor increases in response to (and amplifies) warming. Climate models, which will be discussed below, include this and other feedback loops.

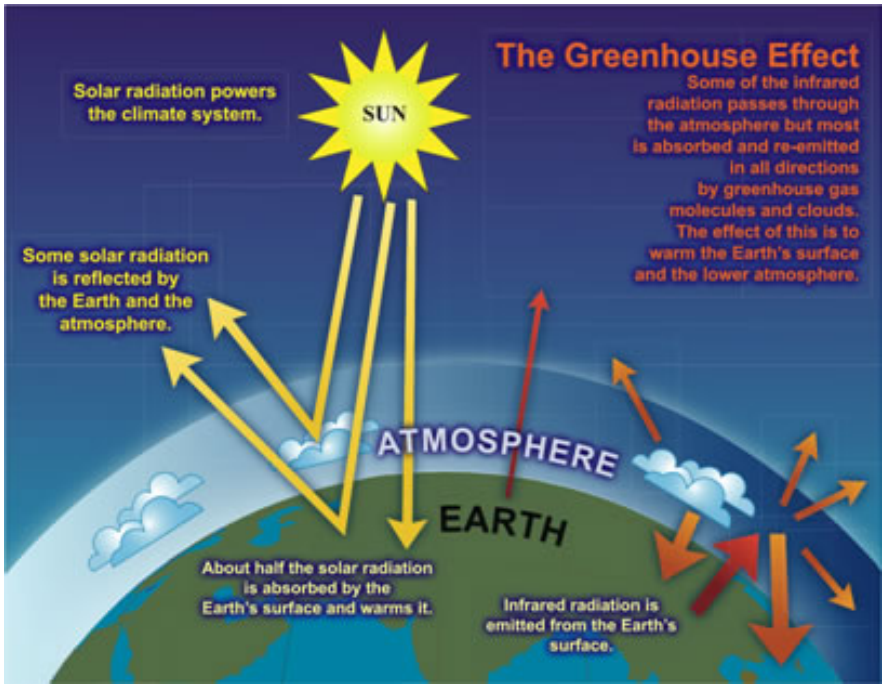

Figure 2: The Greenhouse Effect

Figure 2 illustrates the natural and enhanced greenhouse effect. Greenhouse gases are, for the most part, transparent to incoming solar (shortwave) radiation. When incoming solar radiation reaches the surface of the earth, the radiation warms the earth. The earth's surface then emits this absorbed solar radiation as infrared (longwave) radiation. Atmospheric GHGs absorb this infrared radiation, and in turn re-emit it in all directions. It follows that an increase in the atmospheric GHGs leads to an increase in the heat re-emitted by them, warming the earth (Kiehl and Trenberth 1997).

Discussions about the climate often use the concept of an "anomaly" to quantify changes. An anomaly, as used when discussing climate change, means the departure from a reference value or a long-term mean (average). This most often takes the form of the difference between a current or future value, and the same value during some previous time period. A positive anomaly indicates the quantity of interest is higher than the reference value; a negative anomaly indicates the quantity of interest is lower than the reference value. For example, one might compare the difference between the average global temperature for the year 2012, and the average global temperature for the years 1901–2000 (in this case the temperatures for all the years 1901–2000 would be averaged, and this would be the reference value). The difference between the 1901–2000 average (the reference value) and the 2012 value would be the anomaly.

Ocean Acidification

In addition to the projected climate impacts of increased atmospheric GHGs, an increasing atmospheric CO_2 concentration has changed (and will continue to change) the chemistry of ocean waters, making them more acidic. This increase in acidity (i.e., a lower pH) is known as ocean acidification. Changes in ocean pH may have important biological effects. Marine organisms known as calcifiers rely on the process of calcification to build and maintain their hard body parts. Such organisms include shellfish, corals, and some plankton.

In the simplest terms, the chemical equation that controls the calcification rate is shown below:

$$CO_3^{2-} + Ca^{2+} \Leftrightarrow CaCO_3$$

In a more acidic environment, carbonate ions (CO_3^{2-}) are not as plentiful and the equation above moves to the left (away from $CaCO_3$, a key component of hard body parts). This leftward movement implies that calcifiers may have difficulty building or maintaining their hard body parts.

The overall chemistry involved in this process is shown in Figure 3 below. Longer arrows indicate reactions that are enhanced by an increase in the atmospheric CO_2 concentration. Note that as ocean acidity increases (denoted by

an increase in H^+ ions), H^+ ions combine with CO_3^{2-} (carbonate ions) to produce bicarbonate ions. As a result, fewer carbonate ions are available to calcifiers.

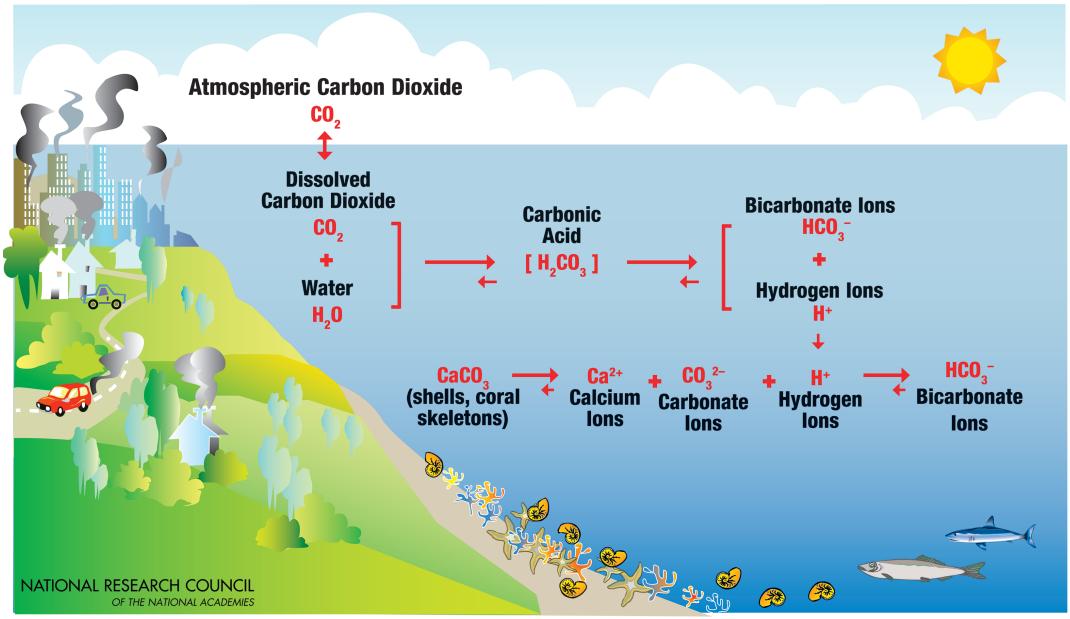

Figure 3: Ocean chemistry, illustrating the effect of elevated atmospheric CO_2. Longer arrows indicate reactions that are enhanced by additional atmospheric CO_2. As acidity increases (more H^+ ions), fewer carbonate (CO_3^{2-}) ions are available to calcifiers for construction and maintenance of their hard body parts.

Greenhouse Gases

Historical Greenhouse Gases

One of the most used methods for determining the historical atmospheric concentration of CO_2 is known as ice core analysis (Barnola et al. 2003; Etheridge et al. 1998; Neftel et al. 1994). The layers of ice and snow (and the air bubbles trapped in the layers) provide a record of the atmosphere going back hundreds of thousands of years. Long, vertical cores are drilled down through ice sheets or glaciers and the air bubbles trapped within are analyzed for gas concentrations.

Recent research has been able to quantify the atmospheric concentration of CO_2 going back about 800,000 years. Figure 4 below illustrates the results from ice core analyses performed in Antarctica. Note how the atmospheric CO_2 exhibits a series of cycles between about 180–300 parts per million (ppm) for the last 800,000 years. Compare these cycles to the current concentration of just under 400 ppm. In other words, the current atmospheric concentration of CO_2 is unprecedented in at least the last 800,000 years. Also note how temperature and the CO_2 concentration are closely related. Recent research confirms that, from a global perspective, increasing CO_2 led increasing temperatures coming out of the last ice age (Shakun et al. 2012).

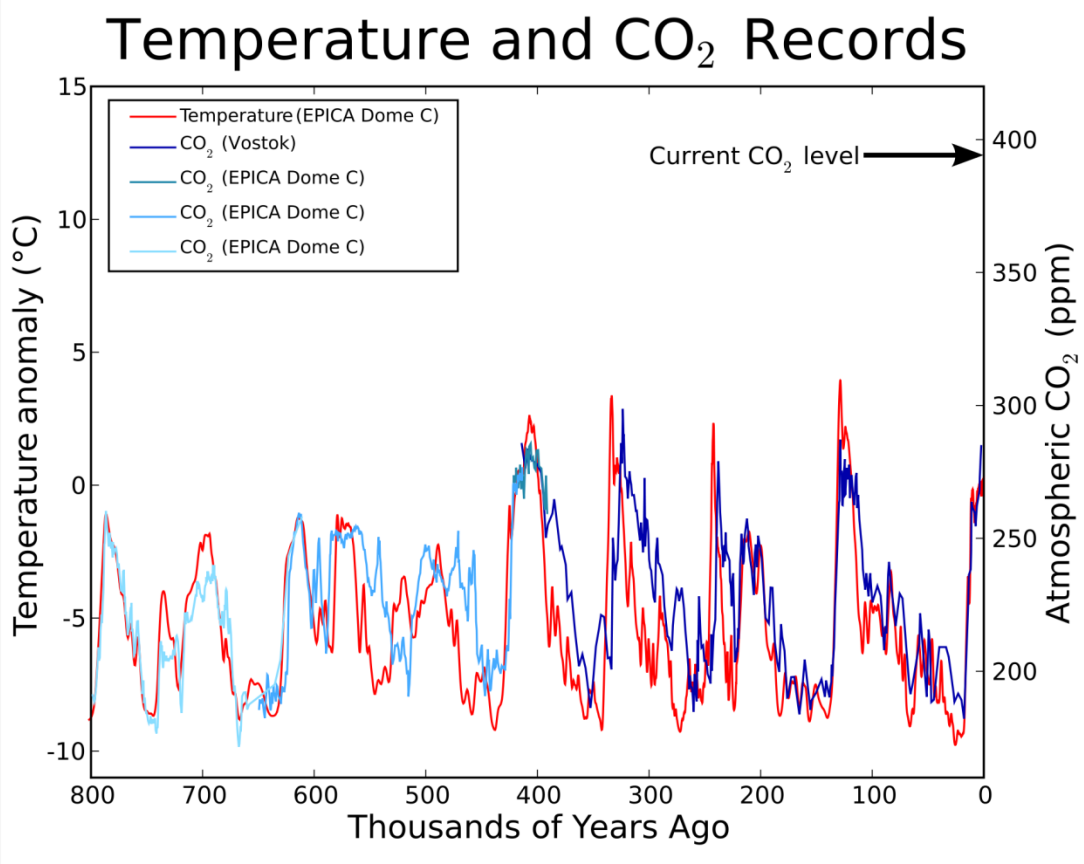

Figure 4: CO_2 from 800,000 years before present. The present time is on the right, at time 0. Note the periodic cycles, and the current level of almost 400ppm, which is much higher than anything seen in the last 800,000 years (Leland McInnis, after Jouzel and Masson-DelMotte 2007; Luthi et al. 2008; Petit 2005; Siegenthaler et al. 2005).

Since 1957, measurements of the atmospheric CO_2 concentration have been carried out from an observing station on top of the Mauna Loa Observatory in Hawaii. Figure 5 shows the results of these measurements. The seasonal cycle of CO_2 is shown by the oscillating red line on the graph. This oscillation is due to the seasonal vegetation cycle in the northern hemisphere (most global vegetation is in the northern hemisphere). As spring begins in the northern hemisphere and the vegetation begins to "green up," CO_2 is removed from the atmosphere by the growing plants. In the northern hemisphere fall (when the vegetation dies off for the winter), the CO_2 concentration rises again. The black line is the running average. Note the steady increase over the last 50+ years.

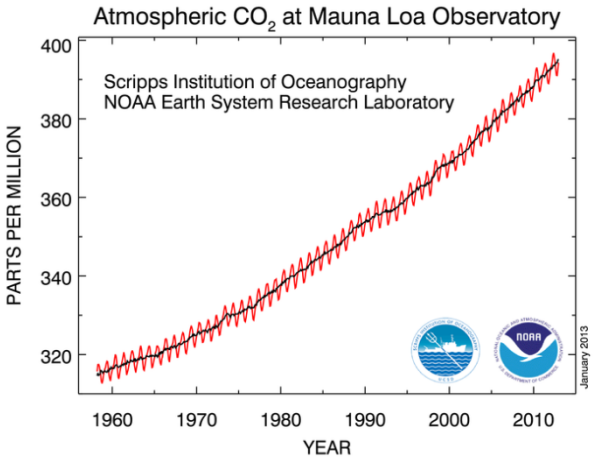

Figure 5: Mauna Loa Observatory, HI, direct CO_2 measurements.

Future Greenhouse Gases

Given the established relationship between GHGs and temperature, in order for researchers to make future projections of climate, there must be some way to quantify the amount of expected future GHGs. Atmosphere-Ocean General Circulation Models (AOGCMs) require a known GHG "forcing" in order to make the calculations for projecting the future climate. This forcing can be thought of as how much effect the GHGs have on the climate: a higher forcing means more effect; a lower forcing means less effect.

To this end, the Intergovernmental Panel on Climate Change (IPCC) developed a suite of future GHG emissions projections (scenarios or storylines). For the most recent (2007) IPCC report, these scenarios are often referred to as the SRESs (Special Report on Emissions Scenarios). Each scenario makes certain assumptions about demographic, social, economic, technological, and environmental developments that would affect GHG emissions. Each scenario was given a name related to attributes of the underlying storylines (e.g., A2, B1, etc.). For the purposes of this report, it is not necessary to understand the details behind each scenario, but it is important to realize what the different scenarios mean in terms of the amount of emissions/forcing (and warming).

Figure 6 illustrates the trajectories of several of the most widely used and discussed scenarios. The gray shaded area represents the range of all possible emissions, while each colored line represents the emissions of a particular "marker" scenario. The black dots represent actual emissions for each year (with the open circle for 2010 being an estimate). Note that actual emissions are within (but at the top of) the range estimated by the IPCC through 2010. After about 2030 the emissions trajectories begin to diverge significantly. When looking out to 2100, the A2 scenario is often used as the "high emissions" future, while the A1B scenario is often used as the "low emissions" future. It should be emphasized that none of these scenarios are predictions of what will occur, but rather are representations of what one future might look like.

It is difficult to know what future GHG emissions will be, and what the exact response (sensitivity) of the climate will be to these emissions (see below). Given this, it is prudent to use a suite of models (i.e., multiple models/emissions scenarios) when considering the future climate.

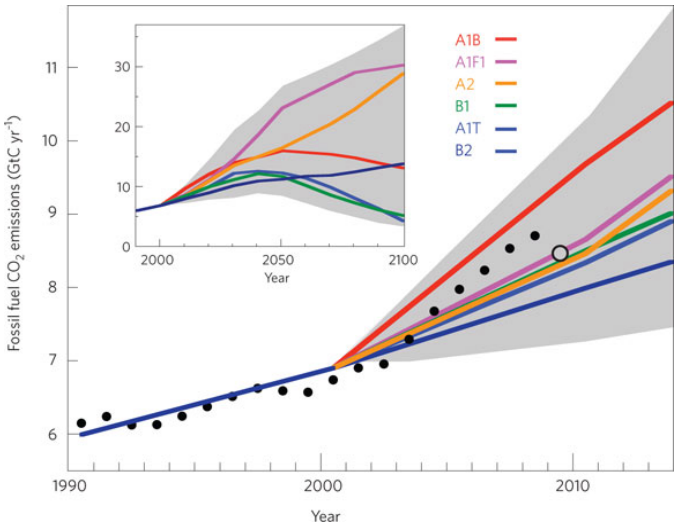

Figure 6: IPCC AR4 SRES emissions scenarios. Each colored line represents one possible future emissions scenario. Black dots on the larger figure are actual emissions; the open circle is an estimate for 2010 (Manning et al. 2010).

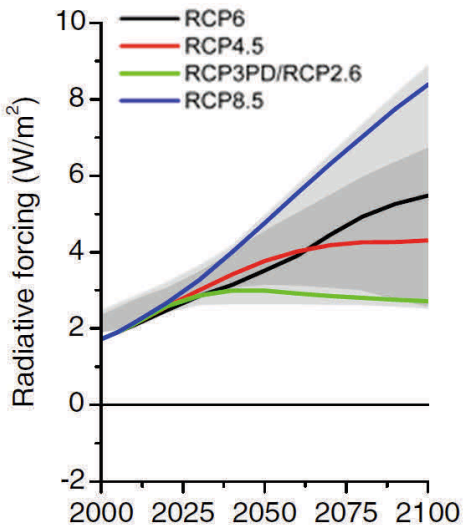

Figure 7: RCP emissions scenarios for the IPCC AR5 (van Vuuren et al. 2011).

For the IPCC Assessment Report 5 (AR5) due in 2013, the representation of the emissions scenarios has changed somewhat. For AR5, four radiative forcing scenarios (or trajectories), known as Representative Concentration Pathways (RCPs), are defined (van Vuureen et al. 2011). While each scenario still represents one possible future, the scenarios are now based on (and labeled in accordance with) the additional radiative forcing that they represent in 2100 (radiative forcing can be thought of as extra energy added to the climate system; in other words, extra heat added to the atmosphere and oceans). A higher radiative forcing corresponds to a higher concentration of GHGs, and a greater degree of warming. The units for the RCPs are watts per square meter (W/m^2).

This additional forcing is with respect to the baseline established in 1750, when there were assumed to be no human influences on the atmosphere. For example, RCP8.5 represents 8.5 W/m^2 of energy added to the atmosphere-ocean system in 2100 as a result of human activities since 1750. The IPCC (AR4) estimates the current additional forcing at about 1.6 W/m^2.

Four RCPs are defined in order to eliminate the notion that a middle pathway is the most likely (i.e., no RCP is considered the "most likely"). Figure 7 illustrates the trajectories of the RCPs in the 21st century. Any value along the RCP trajectory can be used as input to a climate model in order to project possible future climates. As with the older SRESs, no particular trajectory is deemed more likely than another.

The RCPs were developed for AR5 for two primary reasons.

- Their rapid development allowed the climate modeling community to get a "jump start" on the modeling process.
- They allow for parallel development of the socioeconomic storylines that are consistent with the RCPs.

Uncertainty

Three primary sources of uncertainty apply to climate change projections: uncertainty regarding future GHG emissions, natural climate variability, and the uncertainty surrounding the climate sensitivity (Hawkins and Sutton 2009). Each is discussed in turn below.

Future Emissions (Socioeconomic Uncertainty): GHG emissions are largely a function of population, socioeconomic forces, and technology. All of these may in turn be affected by policy choices at all levels of government. Since the interaction of all these components in the future cannot be known with certainty, it is difficult to project future anthropogenic GHG emissions. Societal choice could substantially affect the amount of GHGs added to the atmosphere. As mentioned earlier, climate researchers use a range of possible future emissions to deal with this uncertainty.

Natural Variability (Climate System Uncertainty): Many factors affect the climate and contribute to its natural variability. In the short-term (year-to-year out to a couple of decades), these factors may include volcanic eruptions (which inject particles into the atmosphere that reflect incoming radiation, thereby exerting a cooling influence), and changes in ocean circulation patterns (e.g., the El Niño-Southern Oscillation). In addition, all components of the climate system (the atmosphere, the oceans, and the earth itself) are constantly in motion, leading to constantly changing interactions between them. This variability is an important component of the uncertainty in climate projections. For example, Figure 8 illustrates the inherent variability in annual mean temperature, and the size of the long-term warming trend as compared to this variability (the trend is much larger than the variability). On short timescales, though, the natural variability in the climate can mask (or accentuate) long-term climate trends.

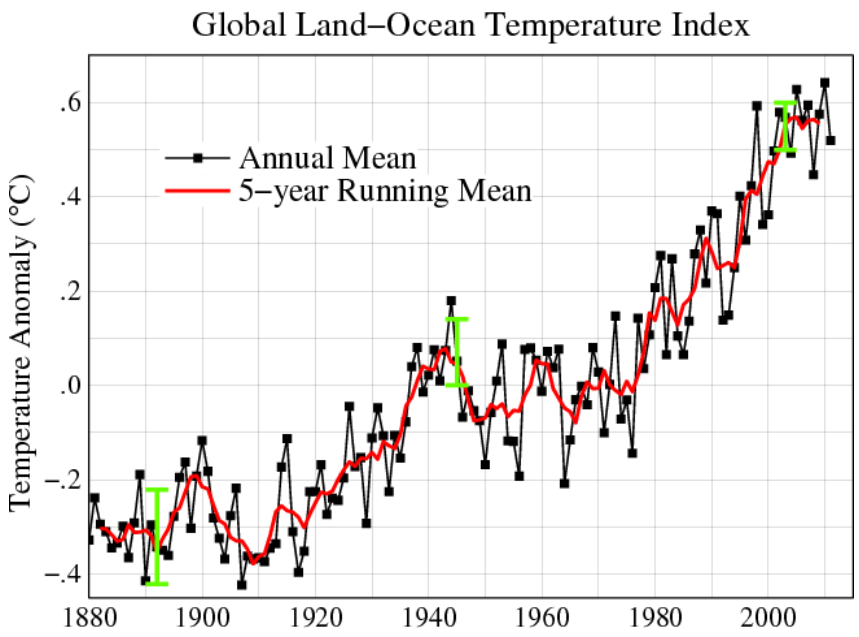

Figure 8: NASA global temperature anomaly (difference between the observed value and a reference value). Green bars are the 2-sigma error estimates (95% CI). The anomaly is relative to the 1951–1980 average (Hansen et al. 2010; NASA GISS). 0.1 °C = 0.18 °F.

Climate Sensitivity (Model Uncertainty): The response of the climate system to an increase of GHGs is the third source of uncertainty in climate projections. The uncertainty of this response stems from uncertainties in the underlying processes (for example, cloud physics). The climate sensitivity, defined as the change in the global temperature due to a doubling of the atmospheric concentration of CO_2, is a convenient measure of the climate's response to GHGs. Figure 9 illustrates the probability distributions of several published climate sensitivities. A higher probability density on the (vertical) Y-axis indicates a higher chance of the climate sensitivity value on the (horizontal) X-axis occurring. As the figure shows, the most likely climate sensitivity is in the range of 2.5–3.5 °C/4.5–6.3 °F per doubling of atmospheric CO_2 concentration. However, a climate sensitivity that is lower or substantially higher cannot be ruled out.

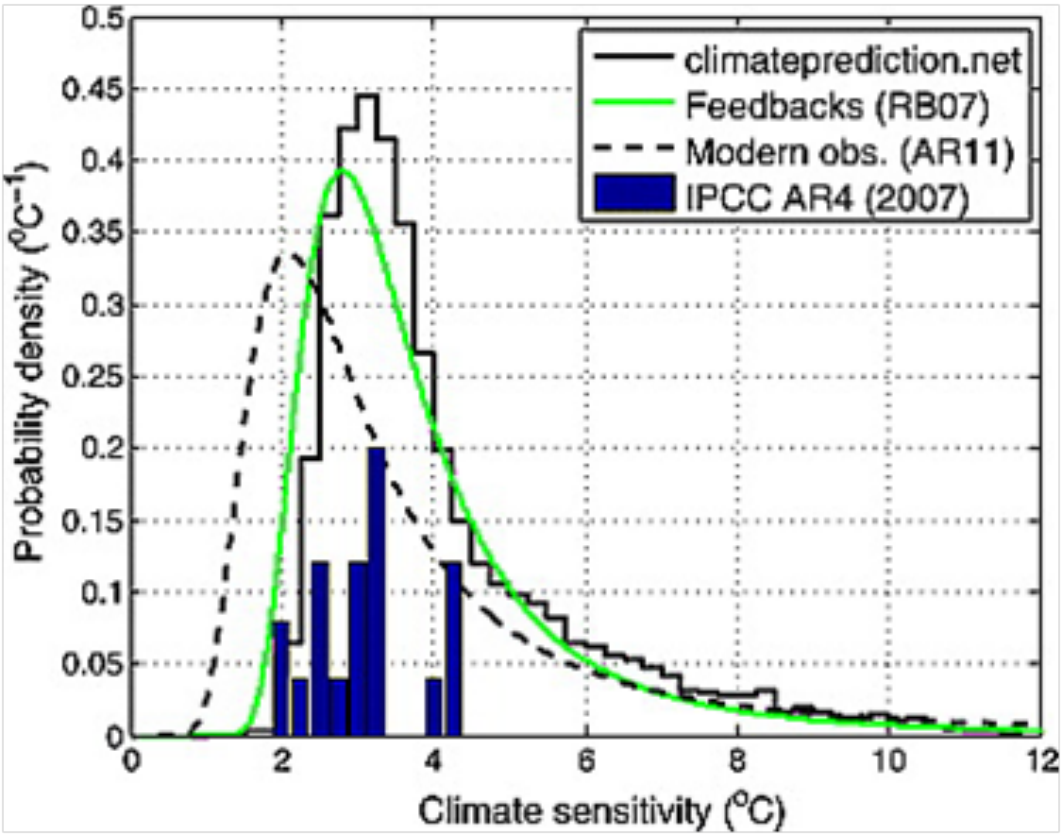

Figure 9: Probability distribution of climate sensitivity (Roe and Armour 2011). The X (horizontal)-axis represents the amount of warming expected if atmospheric CO_2 is doubled over pre-industrial levels (i.e., CO_2 concentration rises to 560 ppm). The Y (vertical)-axis represents the relative probability of a particular climate sensitivity. The blue histogram (from the 2007 IPCC AR4), solid green (Roe and Baker 2007), solid black (climateprediction.net project), and dashed black lines (observations) all represent sensitivity estimates. 1 °C = 1.8 °F.

The above three sources of uncertainty are summarized in Figure 10. This figure illustrates the relative contribution to overall uncertainty of mean temperature from each of the three sources. The left panel of the figure illustrates uncertainty from a global perspective, while the right panel illustrates uncertainty from a regional perspective.

Note that as the lead time increases (i.e., the number of years into the future increases), the uncertainty in GHG concentrations dominates. With shorter lead times, the climate sensitivity of the models is a larger source of uncertainty. For regional projections, natural climate variability can dominate into the first couple of decades. The implication of this is that projecting the effect of increased GHGs on a regional (and even more so, local) level is much more difficult than projecting the effect at the global level.

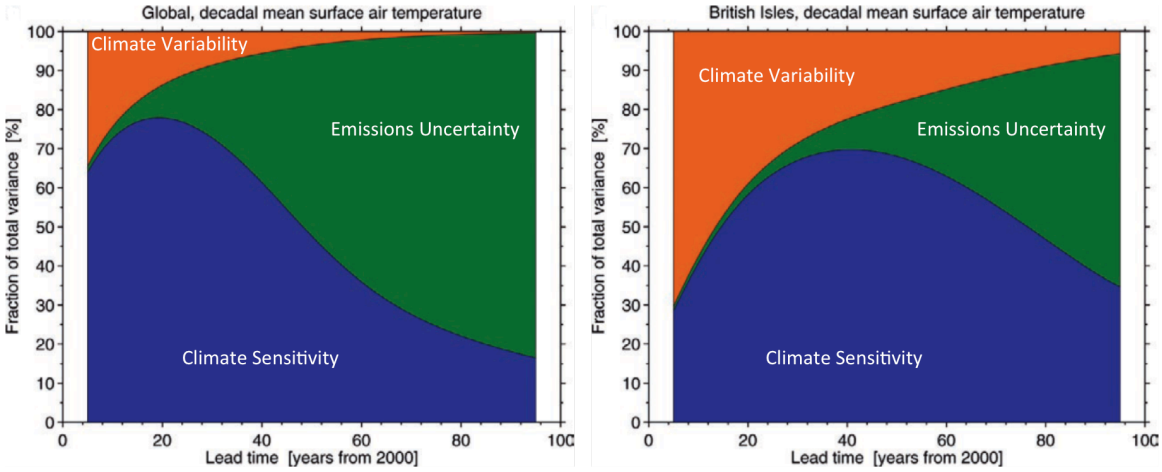

Figure 10: The relative contribution of the three sources of uncertainty as they change with the lead time (i.e., distance into the future) of the projection. Green = emissions uncertainty; Orange = climate variability; Blue = climate sensitivity. The global uncertainty is illustrated on the left; regional uncertainty is on the right. For longer time frames (i.e., further in the future, such as 40 years or more), the climate variability and the climate sensitivity become less important as sources of uncertainty, while the emissions uncertainty dominates (Hawkins and Sutton 2009).

As noted above, any attempt at projecting future climate entails incorporating a number of underlying uncertainties and assumptions into the projection. Using a large number of models (often referred to as an "ensemble") is one way of addressing the uncertainty in projections. The mean, median, percentiles, and spread/range of an ensemble of model projections can give insight into what the future climate might look like. In addition, using multiple permutations of model parameters (emissions scenarios, model sensitivities, etc.), is another way that climate modelers strive to produce a realistic set of possible future climates.

To the degree possible, projections in this report are based on multi-model ensembles and checked for consistency against other climate projections (e.g., Mote and Salathé 2010). Any assumptions made for this project, for example the emissions scenario chosen, are assumptions that could reasonably be expected to occur in the future. In other words, no "extreme" assumptions were made in order to investigate the "edges" of the projection envelope.

Ultimately, the use of climate projections in management decisions has to depend on the time frame of interest and the level of risk tolerance. Any actions taken need to be considered within the context of the inevitable uncertainties. On the other hand, the risks of inaction also need to be part of the decision process.

Historical Trends

Historical Trends at a Glance

Over the past century, the Tillamook Bay Watershed has shown a significant warming trend. Temperatures have risen by 1.0 °F, on average, with the greatest warming happening in the winter. Annual precipitation has decreased very slightly, but has remained relatively constant. Unlike other coastal regions around the planet where sea level is rising, the relative sea level has dropped slightly in the Tillamook Bay Watershed over the past 100 years. Geologic activity off the coast of Tillamook is pushing the coastline upward, accounting for the drop in sea level relative to other regions of the world.

Temperature Trends

Global

As shown in Figure 8 and Figure 11 below, the global temperature anomaly has increased over the last 100+ years.

Figure 11 illustrates the trend in the global historical mean (average) temperature. The left vertical axis (the Y-axis) indicates the difference in mean temperature for each year in the record from the mean global temperature for the 30-year period 1961–1990. The right Y-axis indicates the actual estimated temperature. The black dots indicate the value on a year-by-year basis, while the heavy blue line is the "running average" of the black dots. The blue shaded area around the running average can be thought of as the "margin of error" associated with the running average (the margin of error in this case may be due to missing data and/or measurement inaccuracies). Individual yearly values are allowed (and expected) to be outside the shaded area due to the fact that the shaded area (the margin of error) applies only to the average of the yearly values. The colored lines are fitted to the data ("overlayed" in order to produce a trend line) over various periods: 25, 50, 100, and 150 years. The colored lines give an estimate of the overall trend in mean temperature over the specified time frame. As can be seen from the figure, the rate of warming ranges from about 0.045 °C/0.081 °F per decade over a 150-year period (0.675 °C/1.215 °F over the whole 150-year period) to 0.177 °C/0.319 °F per decade over a 25-year period (0.442 °C/0.796 °F over the whole 25-year period). Note that the rate of warming has increased in recent years (i.e., the trend is accelerating).

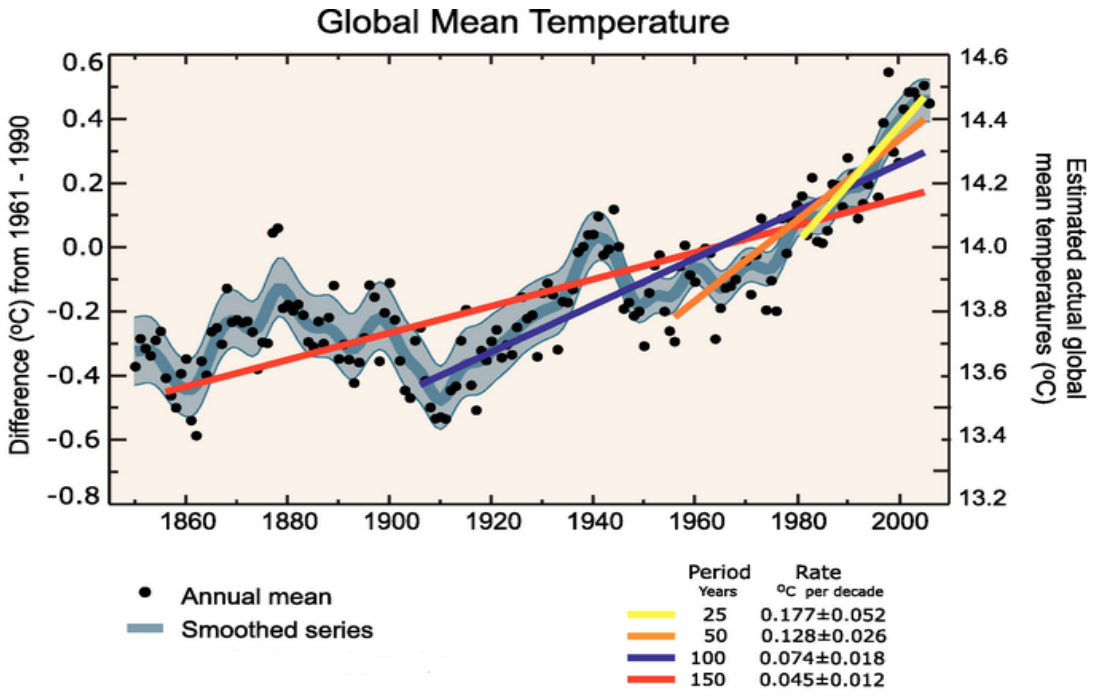

Figure 11: The global temperature anomaly relative to the 1961–1990 reference period. Black dots are the observed values; the heavy blue line is the average of the observations; the gray shaded area is the margin of error. Colored straight lines represent the linear trend over selected periods (Solomon et al. 2007). 0.1 °C = 0.18 °F, 14.0 °C = 57.2 °F.

Regional and Tillamook Bay Watershed Means

The temperature (T) and precipitation (P) data illustrated in Figures 12–15 below are from the US Historical Climatology Network (USHCN). The USHCN is a high-quality data set of daily and monthly records of basic meteorological variables from 1218 observing stations across the 48 contiguous United States. This report uses monthly data (i.e., data aggregated to a monthly quantity) back to 1901 and daily data (i.e., data available on a daily basis) back to 1948. USHCN data are a smaller, high-quality subset of the National Weather Service Cooperative Observer Program (NWS COOP) network data. USHCN monthly data are adjusted for time of observation bias, any station moves, conversion to modern instrumentation and urban heat island effect (Menne et al. 2012).

The USHCN stations from Tillamook 1W (1 mile west of Tillamook), Astoria Airport, and Newport were used for the trends analysis. The stations were chosen because of their location on the northern Oregon coast, and because they are relatively homogeneous in their ocean-influenced climates. Trends are presented for the three-station mean using linear regression.

Temperature data for the Tillamook 1W, Astoria Airport and Newport stations for the historical period (1901–2009) were accessed from the USHCN website (http://cdiac.ornl.gov/epubs/ndp/ushcn/access.html). Monthly temperature data were seasonally and annually averaged; precipitation data were summed by season and year. For purposes of this analysis, climatological seasons were used (Dec to Feb=Winter; Mar to May=Spring; Jun to Aug=Summer; Sep to Nov=Fall). Station data are plotted annually and seasonally. Trends were determined using a simple linear regression and presented as a decadal value (Table 1). Daily precipitation data for 1948–2009 were downloaded for an analysis of daily extreme precipitation (Figure 16). Extreme precipitation was determined using a percentile approach. For this report, the 99th and 99.7th percentile values were chosen to define an

extreme 24-hour precipitation total for the Tillamook 1W station. Trends in number of events over time were also determined by fitting the data with a simple linear regression.

Table 1 below illustrates the trends in overall mean, mean maximum, and mean minimum temperatures over the historical period. Table 1 is an ensemble mean for the three stations (i.e., data for the Tillamook 1W, Astoria Airport, and Newport stations are all included in the analysis). Values in **BOLD** are statistically significant. There has been a statistically significant warming trend, with the greatest warming occurring in the winter.

	Winter	Spring	Summer	Fall	Annual
Maximum Temperature	**0.25**	0.04	0.04	**0.09**	**0.10**
Mean Temperature	**0.10**	0.05	**0.10**	0.01	**0.09**
Minimum Temperature	**0.14**	0.00	**0.16**	-0.06	**0.07**

Table 1: Temperature trends for the Tillamook1W/Newport/Astoria, °F/decade. **Bold** = statistically significant ($p<0.05$).

Figures 12–14 illustrate the historical temperature data for the three stations. In all figures, the green, blue, and orange lines represent the individual stations, while the irregular red line is the average of all three. The straight red line is the linear trend of the data (trend values are detailed above, in Table 1). The top panel in each figure is the annual mean, while the bottom panel illustrates the seasonal means. “Mean Temperature” (Figure 12) is the average temperature during the year/season; “Maximum Temperature” (Figure 13) is the average high temperature during the year/season; “Minimum Temperature” (Figure 14) is the average low temperature during the year/season.

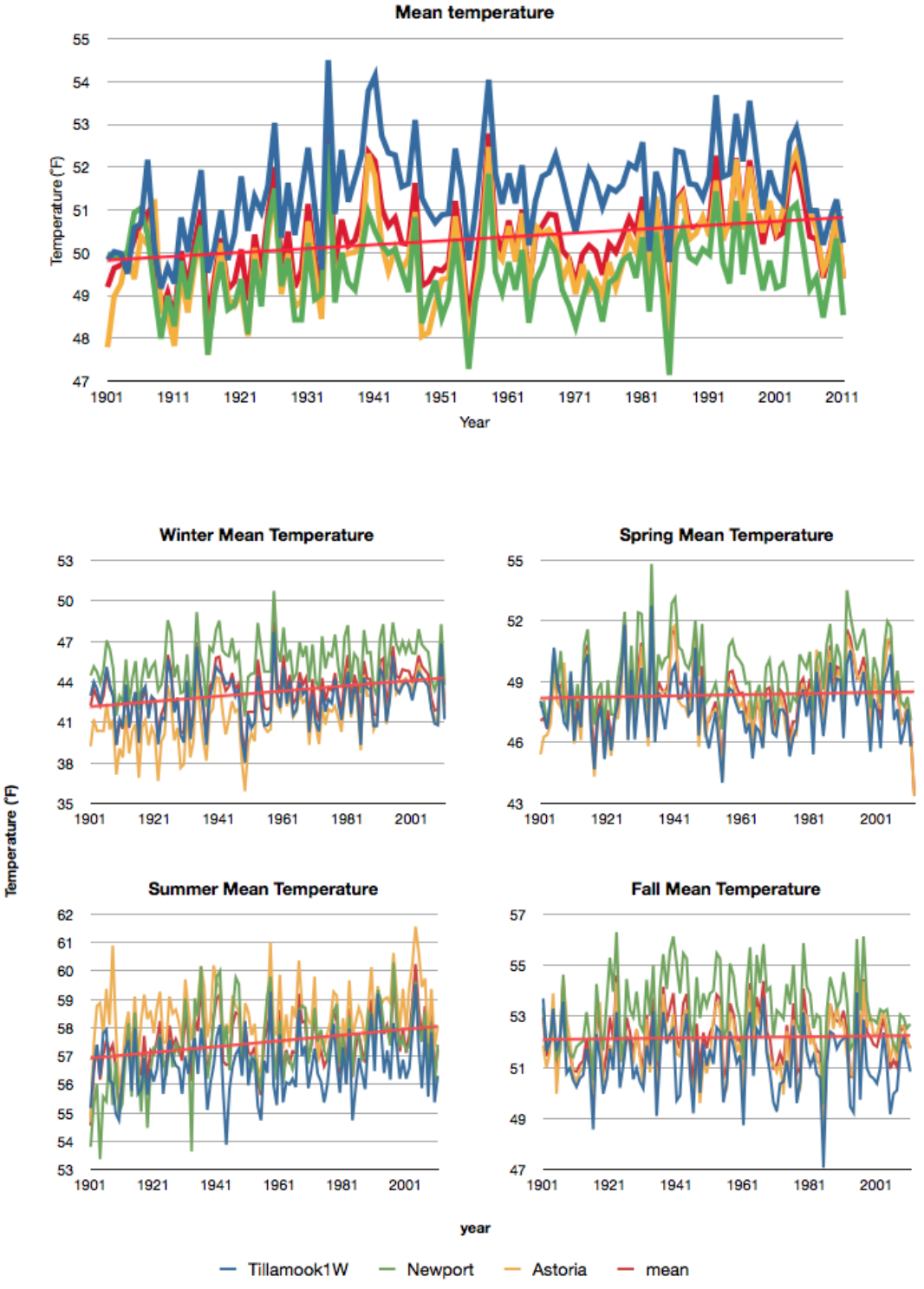

Figure 12: Annual (top) and seasonal (bottom) trends for mean temperature for the Tillamook 1W, Astoria Airport, and Newport USHCN stations.

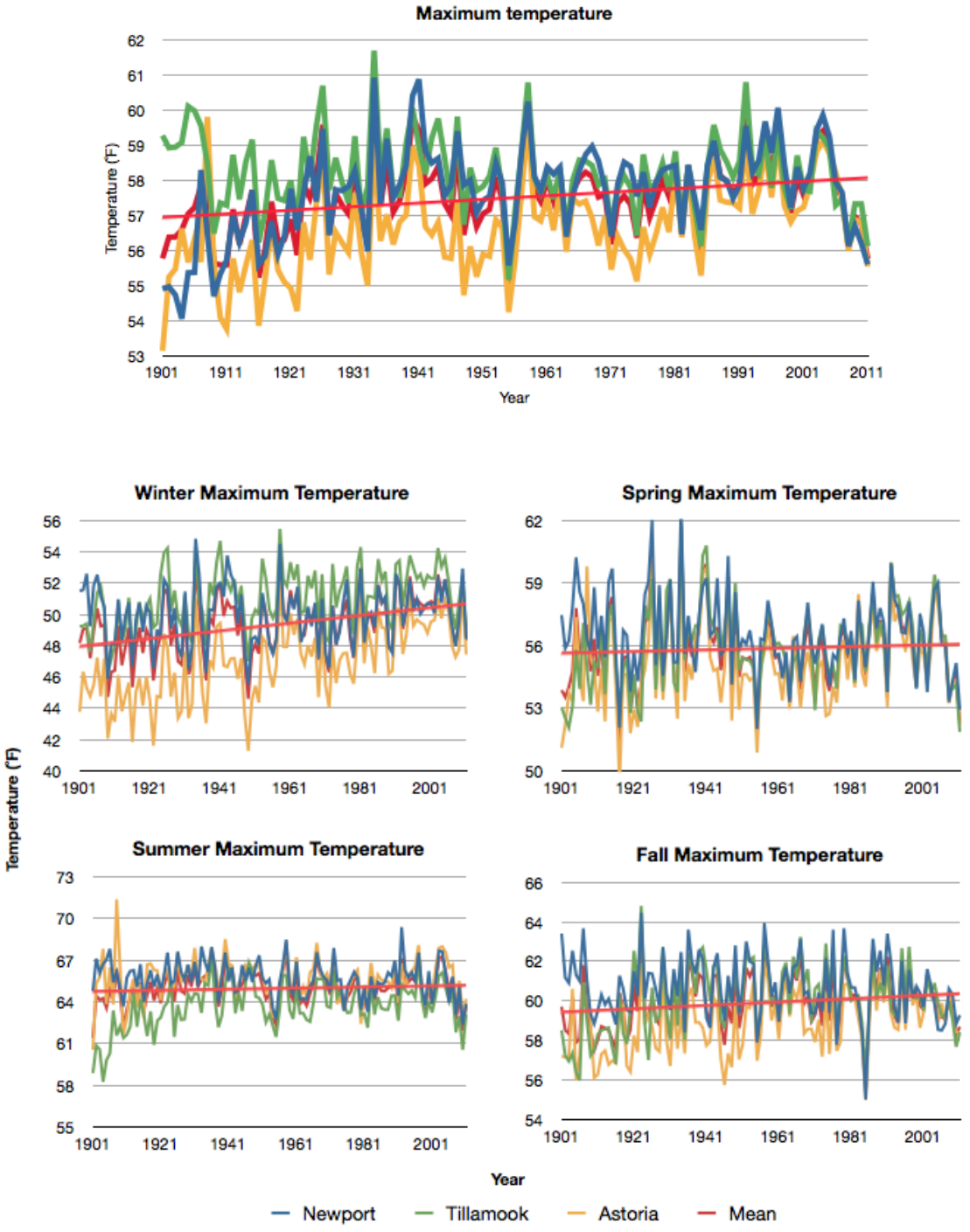

Figure 13: Annual (top) and seasonal (bottom) trends for mean maximum temperature for the Tillamook 1W, Astoria Airport, and Newport USHCN stations.

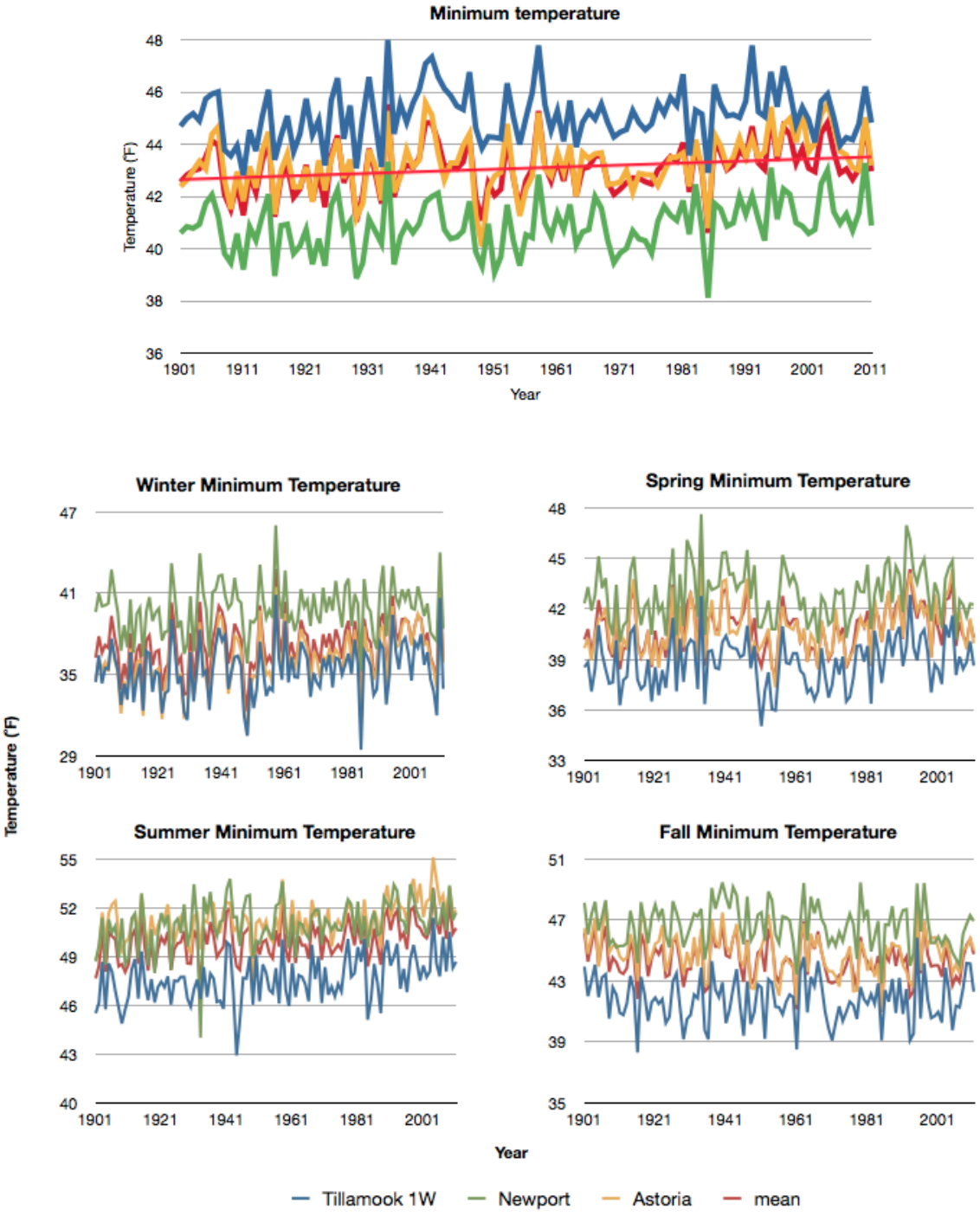

Figure 14: Annual (top) and seasonal (bottom) trends for mean minimum temperature for the Tillamook 1W, Astoria Airport, and Newport USHCN stations.

Precipitation Trends

Global

Global precipitation is highly variable both in time and space. Trends in global precipitation are not as clear as those for temperature. Some datasets show no statistically significant change in global precipitation; and those that do exhibit statistical significance have large uncertainties. In any case, the precipitation in the tropics dominates the global mean (Trenberth et al. 2007).

Regional and Tillamook Bay Watershed Means

Table 2 below describes the annual and seasonal trends in precipitation for the region. The seasons are as before for temperature (i.e., Dec to Feb=Winter; Mar to May=Spring; Jun to Aug=Summer; Sep to Nov=Fall). The values are the mean of the three stations (Tillamook 1W, Astoria Airport, Newport). The tabular values represent how much the annual or seasonal total precipitation value has changed per decade. In this case, for instance, the annual total precipitation has decreased 0.18 inches/decade. In other words, over the course of a century, there has been a decrease in the average amount of precipitation in a year of about 1.8 inches. However, there are no statistically significant trends.

	Winter	Spring	Summer	Fall	Annual
Precipitation	-0.18	-0.18	0.03	-0.18	-0.18

Table 2: Precipitation trends for Tillamook 1W/Newport/Astoria, inches/decade.

Figure 15 illustrates graphically the historical precipitation for the Tillamook 1W, Astoria Airport, and Newport stations. The seasons are as before for temperature (i.e., Dec to Feb=Winter; Mar to May=Spring; Jun to Aug=Summer; Sep to Nov=Fall). Again, the “mean” values are means of all three stations.

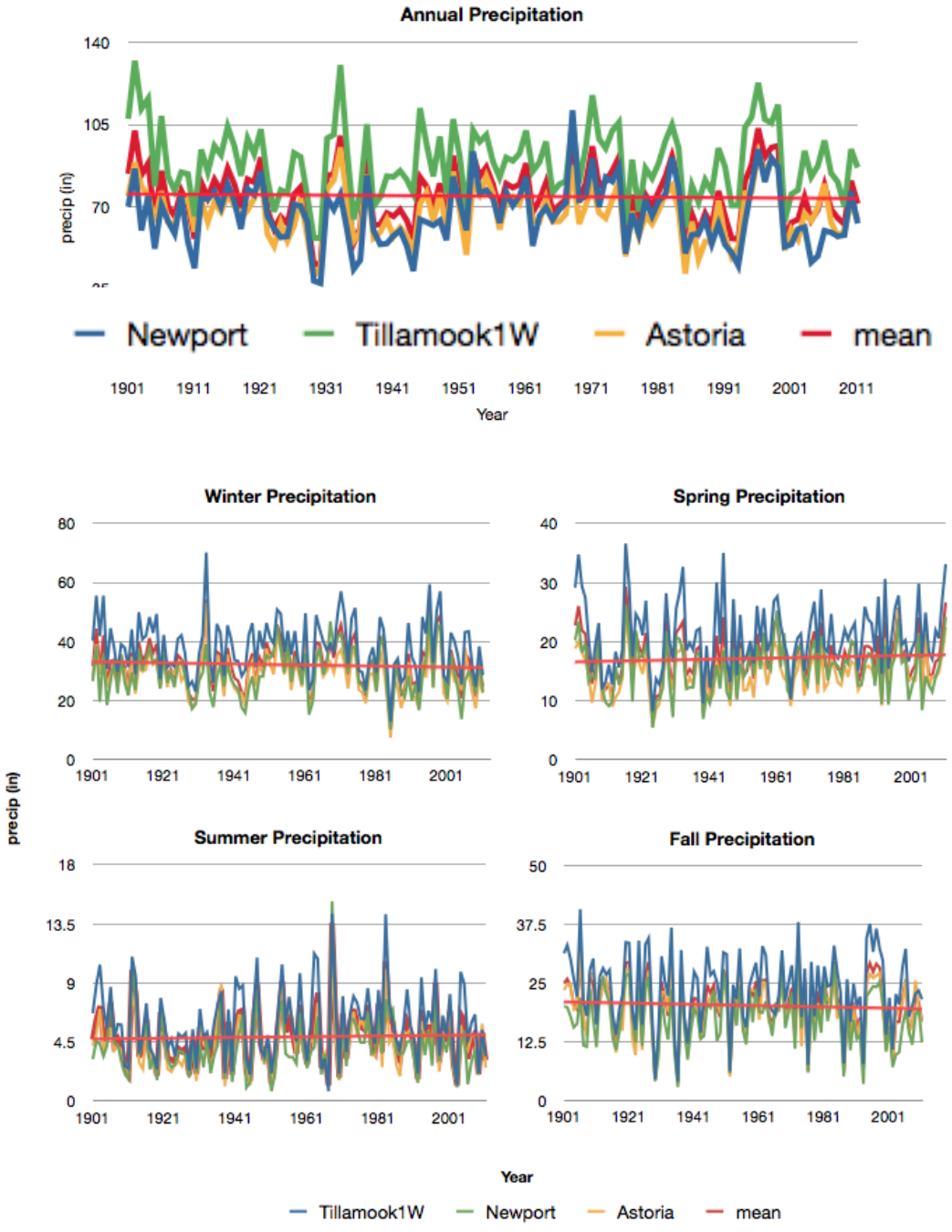

Figure 15: Annual (top) and seasonal (bottom) trends for mean precipitation for the Tillamook 1W, Astoria Airport, and Newport USHCN stations. Values are the total precipitation for the year or season.

Tillamook Bay Watershed Extremes

Figure 16 illustrates extreme precipitation event data from the Tillamook 1W USHCN station. The top panel illustrates the number of precipitation events/year with ≥ 2.10 inches accumulation in a day (the 99th percentile). The bottom panel is similar, except using a threshold of 2.99 inches accumulation in a day (the 99.7th percentile). For the 99th percentile (2.10 inches), the trend has been for an additional 0.05 events/decade. For the 99.7th percentile (2.99 inches), the trend has been for an additional 0.1 events/decade.

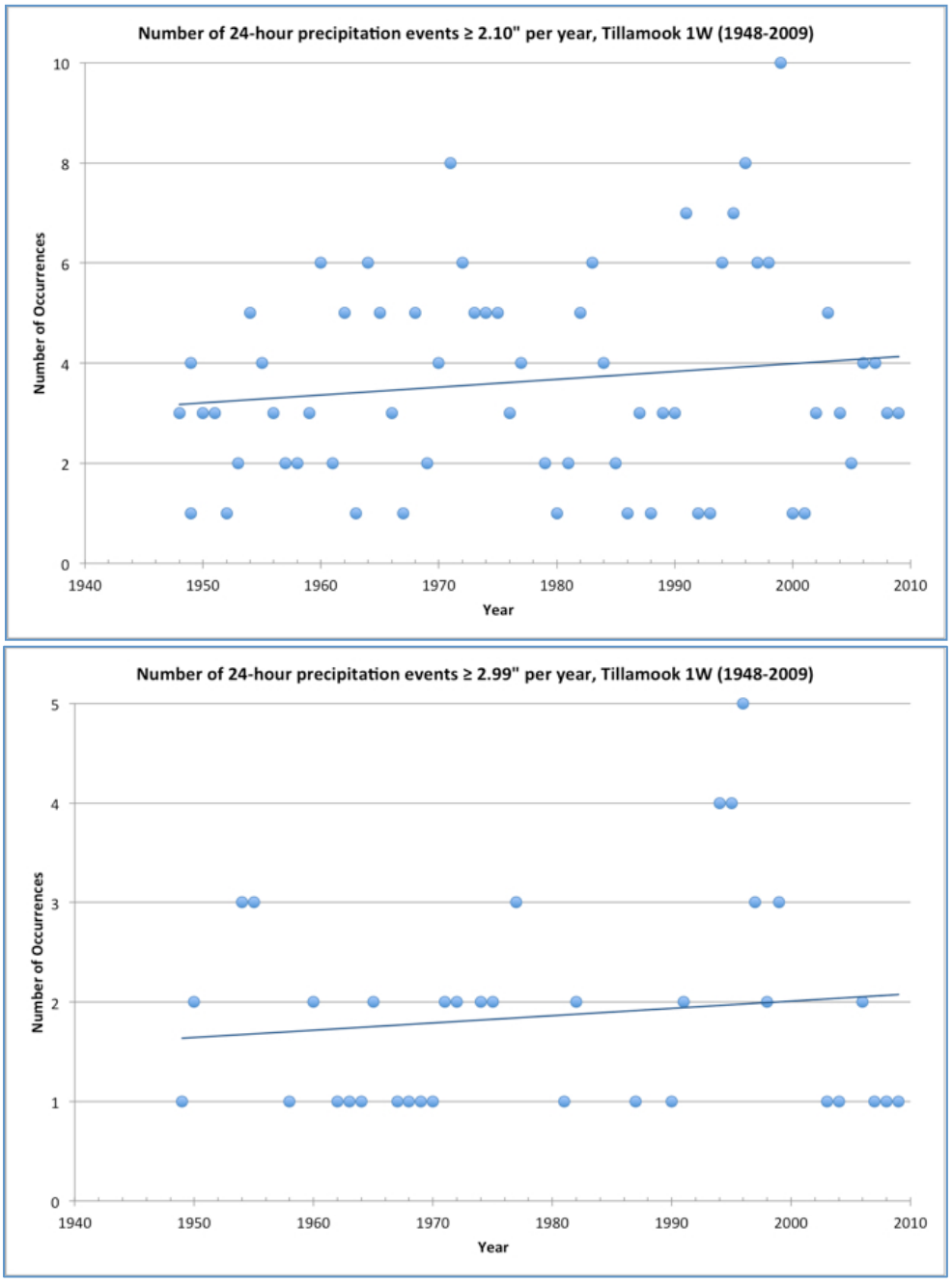

Figure 16: Tillamook 1W extreme precipitation. Number of events/year exceeding the 99th percentile (top), and 99.7th percentile (bottom).

Sea Level Trends

"Sea level," in the context of examining climate change, really consists of two components: the global average sea level; and the sea level experienced at any point along the coast (the local sea level). As will be shown below, global and local sea level trends can be quite different.

The apparent change in sea level at a particular coastal location is known as the "relative change in sea level". It is known as "relative" because it is relative to fixed locations on the shore. A rising relative sea level means that rising water is covering more of the shoreline; conversely, a falling relative sea level means that more of the shore is becoming exposed.

Relative sea level change has two components: the changes in absolute global sea level; and local changes that may work in concert with, or oppose, the changes in global sea level. Relative sea level change is the sum of both of these components (either component may be positive or negative). Below, each of these processes will be examined in detail.

For example, if the absolute global sea level rises by 1.8 mm in a particular year, but local tectonics (see below) cause the land surface to rise by 0.5 mm that year, the relative sea level rise in that location will be only 1.8 – 0.5 = 1.3 mm.

Global Sea Level

Sea level has varied significantly over the earth's history. While the instrumental record (via tide gauges) only goes back to the 1800s, proxy data (i.e., data that can be used to indirectly estimate sea level, such as cores drilled from salt marsh sediments) has been used to estimate global sea level back 2,000 years. In addition, semi-empirical models (i.e., models based on both observations and theory) have also been used to approximate historic sea level. Figure 17 (NRC 2012) shows a reconstruction of sea level based on proxy sea level data, a semi-empirical model, and instrumental data when it became available. From the figure, it can be seen that the recent rate of sea level rise is unprecedented over the last 2,000 years. The recent portion (the last 100–150 years) of this figure will be discussed in more detail below.

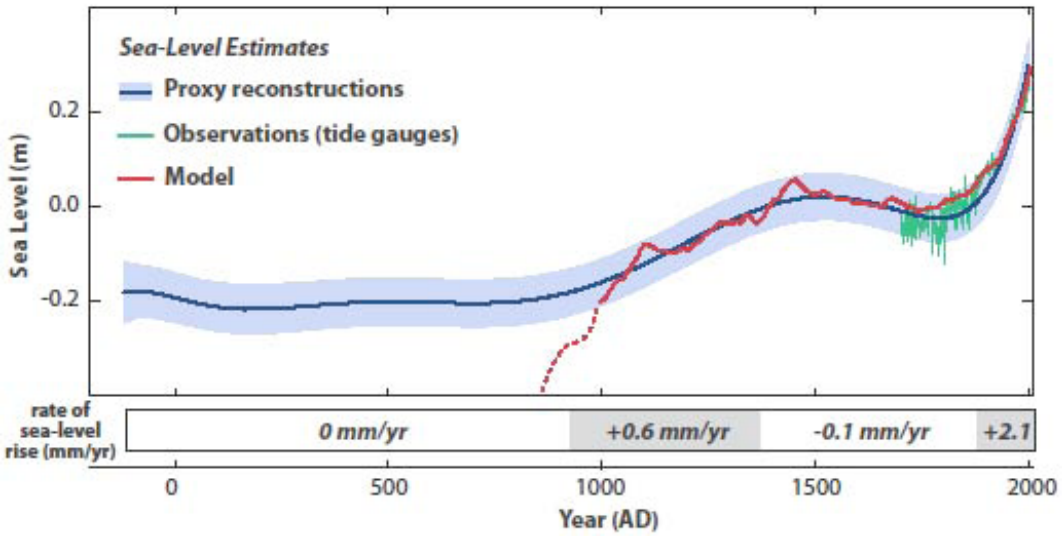

Figure 17: Global sea level estimate. Proxy reconstructions use indirect data (such as sediment cores) to estimate sea level. "Model" refers to a semi-empirical sea level model. The dotted red line indicates where the model deviates from the proxy reconstruction (NRC 2012).

Global sea level is affected by several processes (Bindoff 2007):

- Thermal expansion of sea water (water expands when it warms).
- The addition of water to ocean basins as ice on the land (mountain glaciers and ice sheets) melts.
- The transfer of water between terrestrial reservoirs and the ocean. Water withdrawn from aquifers eventually ends up in the ocean, raising sea level. However, water stored behind dams (impoundment) will lower sea level.

Of these processes, the first and second account for the majority of the changes measured in global sea level recently. The third process is difficult to quantify, but the net effect is thought to contribute little to the recent changes in sea level (NRC 2012).

Figure 18 illustrates changes in global mean sea level since the late 19th century. From the figure it is apparent that global mean sea level has risen on the order of 170mm/6.7inches over the 20th century. The IPCC (2007) also calculated the rate of sea level rise for different time periods (Table 3)*. They note that there is considerable decadal variability in the rate of sea level rise. It is not known if the increased rate of the last few decades is a long-term trend or due to natural decadal variability.

*Previous IPCC (2007) estimates were that for the years 1961–2003 thermal expansion accounted for about 25% of observed sea level rise, and the melting of the land ice accounted for about 40%. However, the sum of the estimates for each of the three processes contributing to global sea level rise over this period is substantially (35%) below the observed sea level rise. For the years 1993–2003, thermal expansion accounted for about 50% of observed sea level rise, with melting ice accounting for about 40%, and the discrepancy between observed sea level rise and the sum of three contributing processes was only about 10%.

Since the publication of the 2007 IPCC report, the attributions in the previous paragraph have been revisited as a result of a bias discovered in some of the data. The end result is that the contribution of thermal expansion to recent sea level rise has been reduced, while the contribution of melting land ice has increased. Specifically, since 2006 the rate of ice loss from the Greenland Ice Sheet has increased, and Antarctic ice is now assumed to contribute (via melting) to sea level change, whereas before it was reducing sea level rise by accumulating water (as snow and ice). The net effect is that in the most recent published estimate for sea level rise from 1993 to 2008, melting land ice accounted for about 65% of the total (Church et al. 2011).

Time Period	Rate of Sea Level Rise
20th century	1.7 ± 0.5 mm/year
1961–2003	1.8 ± 0.5 mm/year
1993–2003	3.1 ± 0.7 mm/year

Table 3: Rate of sea level rise.

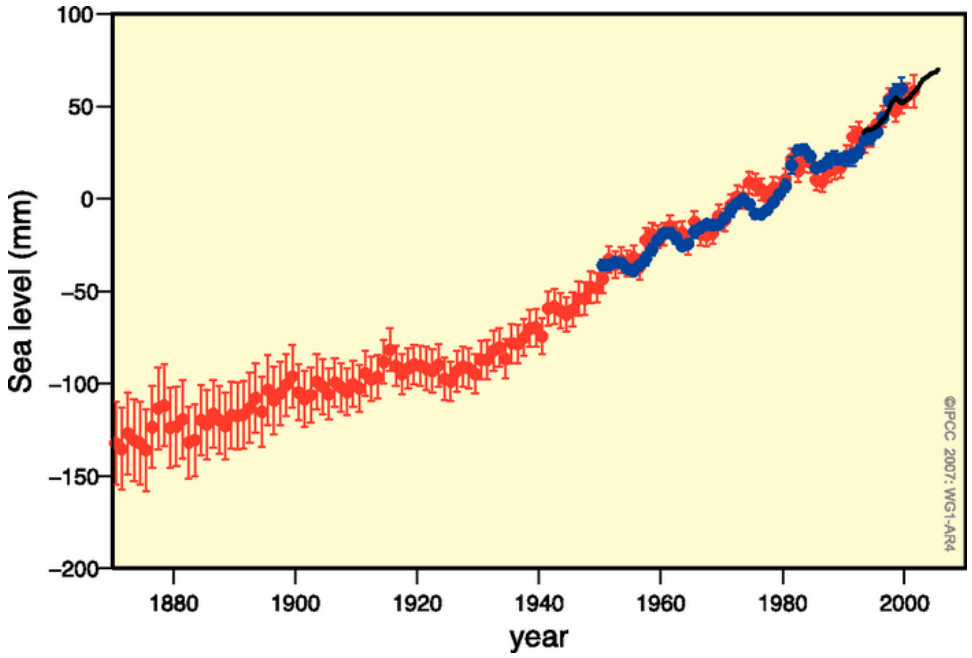

Figure 18: Change in sea level. Red and blue data points are based on tide gauge measurements from 1950; black data points are satellite altimetry data. Units are the deviation relative to the 1961–1990 mean (for the tide gauges) or the 1993–2001 mean (for the satellites) (Bindoff 2007).

Regional Sea Level

As mentioned above, the relative sea level along the coast of Oregon is the sum of changes in the global sea level, as well as any local effects that may impact sea level. For a location on the coast such as the Tillamook Bay, the primary local effects include: changes in ocean circulation and regional climatic conditions, vertical land motion, and gravitational effects from melting ice. Each of these effects is discussed below.

The El Niño-Southern Oscillation (ENSO) and the Pacific Decadal Oscillation (PDO) are quasi-periodic climate patterns which occur on the period of every few years for ENSO, and a range of timescales for the PDO. Both the ENSO and the PDO have "warm" and "cool" phases. A warm phase for either one of them tends to raise sea level along the west coast, while a cool phase tends to lower it. For example, a strong El Niño may increase sea level 10–30 cm/3.9–11.8 inches for several months in the winter. ENSO and the PDO together combine to produce significant variability in seasonal to decadal sea level trends in the Pacific Northwest (NRC 2012). Seasonal variations in sea level are also quite important, with an average difference in sea level of about 23.5 cm/9.25 inches at the Astoria tide gauge between August (low) and January (high).

In the Pacific Northwest, vertical land motion is a result of two processes: plate tectonics and glacial isostatic adjustment (GIA). The Oregon coast is in a tectonically active area: the Juan de Fuca and Gorda plates are colliding with (and being subducted under) the North American plate (Komar et al. 2011). This tends to elevate the coastal land surface as the North American plate "rides up and over" the oceanic plates. This reduces rates of relative sea level rise for the west coast north of Cape Mendocino, California (when compared to global values). GIA occurs when land that was formerly compressed under large masses of ice rebounds as the ice melts. For the areas formerly under a large mass of ice (such as northern Washington) this results in uplift. For areas on the ice margin and beyond, such as the northern Oregon coast, GIA is causing a subsidence in the land surface (NRC 2012).

In addition to increasing the volume of ocean water, a large amount of melting land ice changes the earth's gravitational field as the mass of the ice is transferred to the ocean, and the earth's crust in the vicinity of the melting deforms. This is known as the "sea level fingerprint" effect (NRC 2012). The result of the sea level fingerprint along the northern US west coast (in the vicinity of Tillamook Bay) is to reduce the apparent rise in global sea level (NRC 2012).

The net effect of all the processes listed above is that the west coast north of Cape Mendocino, California, is rising on the order of 1.5–3.0 mm/yr (effectively reducing relative sea level rise by that amount). This compares to the California coast south of Cape Mendocino, which is subsiding on the order of 1.0 mm/yr or more (effectively increasing relative sea level rise by that amount) (NRC 2012). The rate of vertical land motion, however, can vary markedly within this broad characterization (Komar et al. 2011), resulting in significant differences in relative sea level changes even for locations relatively close to each other. Figure 19 illustrates these local variations in sea level rise.

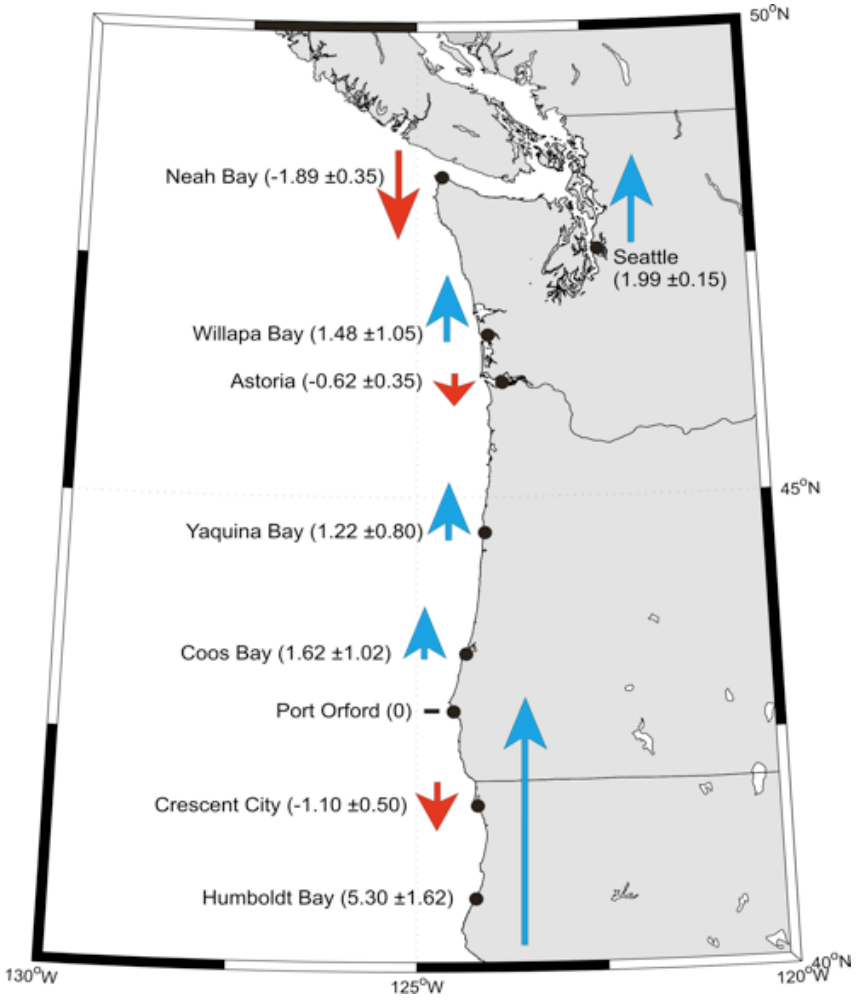

Figure 19: Change in sea level based on analysis of NOAA tide gauges along the coast of the PNW. Colored arrows represent the rates of change in relative sea levels (mm/yr) over the last several decades, along with their uncertainty. Values generated used summer data only in order to minimize ENSO effects (OCAR 2010).

Figure 20 (NOAA SL) below illustrates historical relative mean sea level data for Astoria, Oregon, just north of the Tillamook Bay (Astoria data is used here because it is of much higher quality than data from the gauge at Garibaldi). The data for Astoria shows a mean sea level trend (fall) of -0.31 ± 0.40 mm/yr from 1925 to 2006. Compare this to the global 20th century trend of 1.7 ± 0.5 mm/yr, and the 1993–2003 global trend of 3.1 ± 0.7 mm/yr. The trend value for Astoria in Figure 20 differs slightly from the value in Figure 19 because Figure 20 relies on 12-month data, while Figure 19 uses data only from the summer months.

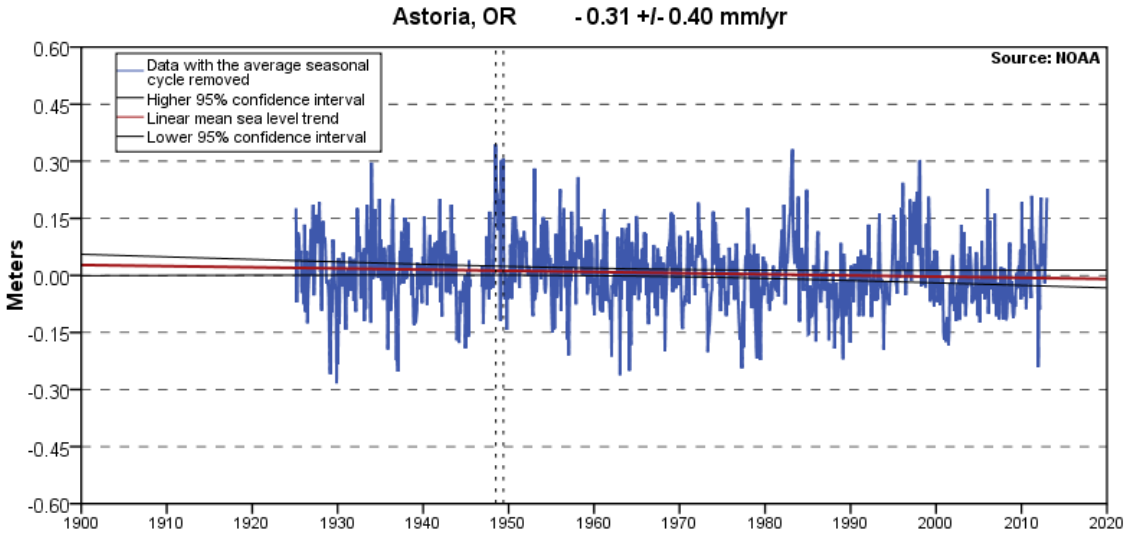

Figure 20: Mean sea level trend, Astoria, Oregon.

Wave Height and Storminess

Data showing increased wave heights and/or storminess in the northeast Pacific is mixed, and the interpretation of this data is controversial. Studies of these effects are hampered by the fact that there are typically only a few decades worth of data, which makes it difficult to distinguish any trends from the considerable natural variability (NRC 2012; Ruggiero et al. 2010).

Snow Days

The ocean-moderated mild climate of the Oregon coast means that snow in the Tillamook area is infrequent, but also not uncommon. USHCN data for Tillamook 1W show 80 days with measurable snow (≥0.01 inches) between 1948 and 2009, or an average of about 1.3 days/year, with an average of 1.67 inches/day. Measuring snow at any location presents a number of challenges; many COOP and USHCN stations no longer report snow measurements. Trends analyses on station snow data are difficult and often ill-conceived due to station temporal inconsistencies introduced by station location, observer, and management practices, and by missing data (Kunkel et al. 2009).

Ocean Acidification

Since the beginning of the Industrial Revolution (~1750), the oceans have absorbed on the order of 127 billion metric tons of carbon (as CO_2) from the atmosphere. This quantity represents about one-third of all the human-generated carbon emissions of the last 250 years (Sabine and Feely 2007). As a result, the pH of the oceans has dropped (i.e., they have become more acidic) by about 0.1 units (Caldeira and Wickett 2005; Feely et al. 2004, 2008; Orr et al. 2005; Sabine et al. 2004).

Regions of the West Coast, including Oregon, have recently been found to be particularly susceptible to ocean acidification (OA), due to the upwelling of deep waters having high carbon dioxide content and low pH (Feely et al. 2008; Hauri et al. 2009). Upwelling systems such as those along the Oregon coast already show pH values that are as low as those expected for most open ocean waters several decades from now. As a result, the Oregon coast will be especially sensitive to ocean acidification (Hauri et al. 2009).

Future Projections

Future Projections at a Glance

Tillamook Bay Watershed is projected to be warmer by between 4 °F and 7 °F by next century. There will be more days above 90 °F on the east side of the watershed, and fewer days with temperatures below freezing. Annual precipitation is projected to increase about 5% by 2100 across the watershed. Although the fall and winter seasons will be wetter under both scenarios, spring and summer will be drier. Summer precipitation could decrease as much as 19%, while spring precipitation may go down as much as 4%. The wettest days are projected to get wetter, and the number of dry days is projected to increase. By 2100, local sea levels could rise about 24 inches, with a possible range of 16–55 inches. Ocean acidification, already high on the West Coast, will be an ongoing concern for the watershed.

Modeling Introduction

Coupled Atmosphere-Ocean General Circulation Models (AOGCMs, or just GCMs), and Global Climate Models (also GCMs) are important tools used for studying the climate. These models rely on mathematical equations to represent the interactions between the atmosphere, oceans, and other components of the global climate system. Sophisticated computer programs employ these equations to simulate the climate.

Climate models typically run on imaginary grids of varying sizes (IPCC 2007). The models calculate the behavior of the climate within each grid cell in order to arrive at an overall picture of climate dynamics. Smaller grid cells (i.e., higher/finer resolution) can be useful for providing more localized climate information. However, smaller grid cells require more computer processing power, storage, and other resources.

Another way to achieve higher spatial resolution (i.e., more localized climate information) is through downscaling relatively coarse spatial information to something finer. For example, one might downscale GCM output based on 1x1 degree (lat/lon) grid cells to smaller grid cells (say 50 km x 50 km). This downscaling may be achieved in one of two ways: statistical downscaling or dynamic downscaling (Bader et al. 2008).

Statistical downscaling methods use correlations among observed and modeled meteorological variables to predict regional and/or local patterns and events that are likely to occur based on the broader-scale GCM simulations.

In statistical downscaling, statistical relationships between observed and modeled climate parameters are developed. These relationships are then applied to future model results in order to generate climate information at higher resolution than the original GCM output. The advantages of statistical downscaling include efficiency and speed. A disadvantage of statistical downscaling is that it assumes past relationships will hold for the future ("stationarity"). This assumption may or may not be true.

Dynamical downscaling involves the use of a high resolution regional climate model "inside" a lower resolution global model. The global model provides the conditions at the boundaries of the regional model. Advantages of dynamical downscaling include an ability to simulate unique (i.e., unanticipated) local conditions into the future (in other words stationarity is not assumed); and, there is no reliance on observations (which may not be available) to develop statistical relationships. Primary disadvantages of dynamical downscaling are the computational resources and expertise required.

Methods

Coupled Model Intercomparison Project 5 (CMIP5) Global Climate Models

This project uses a suite of 13 GCMs from the Coupled Model Intercomparison Project v5 (CMIP5) as the basis for future climate projections. The CMIP5 models will also serve as the basis for the next IPCC Assessment Report (AR5) in 2013. The CMIP5 models provide the most up-to-date projections for future climate, incorporating recent advances in climate science, as well as improved resolution enabled by advances in computing capabilities. Over 20 different modeling groups from around the globe are participating in CMIP5 (CMIP 2012).

The output data from these 13 models have been downscaled using the Multivariate Adaptive Constructed Analogs (MACA) statistical downscaling method (see below). Table 4 details the models used. Model selection was based in large part on the availability of data at a daily interval for the climate parameters identified.

Model Name	Country of Origin
BNU-ESM	China
CanESM2	Canada
CNRM-CM5	France
CSIRO-Mk3-6-0	Australia
GFDL-ESM2G	USA
GFDL-ESM2M	USA
HadGEM2-CC	United Kingdom
HadGEM2-ES	United Kingdom
INM-CM4	Russia
MIROC5	Japan
MIROC5-ESM	Japan
MIROC5-ESM-CHEM	Japan
MRI-CGCM3	Japan

Table 4: CMIP5 Models

Multivariate Adaptive Constructed Analogs (MACA) Statistical Downscaling Method

The MACA downscaling method is a form of statistical downscaling that relies on a library of historical observations to transform coarse resolution GCM output to a spatial scale useful for local impacts assessments (Abatzoglou and Brown 2011). Native resolution for CMIP5 models over land ranges from approximately 1 to 3 degrees of latitude and longitude (about 100–300 km at the latitude of the TBW). In other words, at native resolution, no features smaller than 100–300 km can be resolved. Here, via the MACA process, the coarse GCM spatial resolution has been downscaled to 4 km. So, after downscaling, unique climate data is available for each 4 km x 4 km grid cell in the study area. Figure 21 illustrates the effects of different spatial resolutions over the British Isles. Note the considerable detail that is lost when going from even 25 km resolution to 300 km resolution.

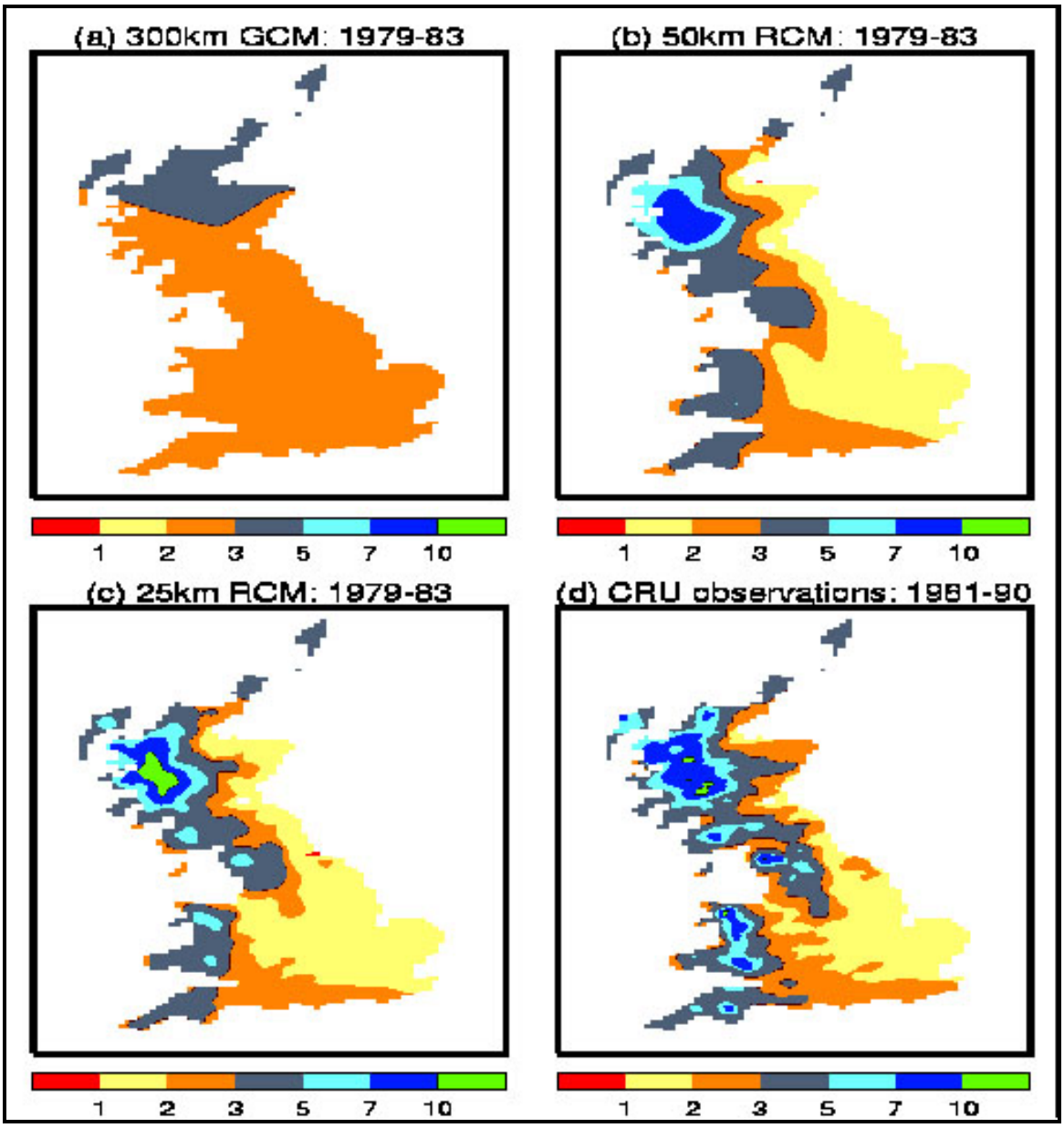

Figure 21: Winter precipitation over the British Isles, average mm/day, as projected by (a) 300 km resolution Global Climate Model, (b) 50 km Regional Climate Model, (c) 25 km Regional Climate Model. Observations (d) at approximately 15 km resolution from the Climatic Research Unit (CRU) of the UK Met Office. 10 km = 6.2 mi.

Emissions Scenarios

The MACA downscaling project chose two CMIP5 emissions scenarios to represent possible emissions futures: RCP4.5 and RCP8.5. In the following projections, RCP4.5 is referred to as the "low emissions" scenario, while RCP8.5 is referred to as the "high emissions" scenario. As stated earlier, neither one of these scenarios should be considered as the most likely scenario. Rather, they should be considered as two of several possible futures.

Historical Modeled Data

A number of the projections below make use of "historical modeled" data. Historical modeled data is generated by the climate model running over the historical period. In other words, the climate model is used to produce a historical data set, instead of using observations (which may be missing or of unknown quality). The goal of historical modeling is not to exactly reproduce the day-by-day weather over the historical period, but rather to reproduce the overall climate statistics (long-term averages) for the historical period. Using historical modeled data allows for an "apples-to-apples" comparison when comparing the climate of the historical period to future projected climate.

MACA Data Averaging and Aggregating

For the overall TBW domain, 96 gridpoints that lie within the TBW domain were included in this analysis. Since MACA data is available at daily intervals (i.e., a daily timestep), an area average was computed for each domain (East or West) for each daily timestep. For time periods other than daily (annual, seasonal, etc.) data was aggregated to the desired quantity.

For temperature, the MACA dataset provides only a daily maximum and minimum. The daily average temperature for this study was approximated as ((Tmax+Tmin)/2).

Several of the projections make use of 30-year "decadal" periods (e.g., 2040–2069). Three decadal periods were chosen in order to give a feel for "near-term" (2010–2039), "mid-century" (2040–2069), and "long-term" (2070–2099) climate change.

Temperature Projections

This section contains temperature projections for both the East and West domains of the TBW. Projections for means and extremes over daily, seasonal, and annual time periods are presented.

Means

Figure 22 illustrates the annual mean temperature for the TBW. Projected warming for both the East and West domains is similar, with about a 9–10 °F increase by 2100 for the high-emissions scenario and 5 °F for the low-emissions scenario. Due to inertia in the climate system, warming rates for the two scenarios are similar until mid-century. It is only after midcentury that the amount of warming begins to differ substantially between the two RCPs.

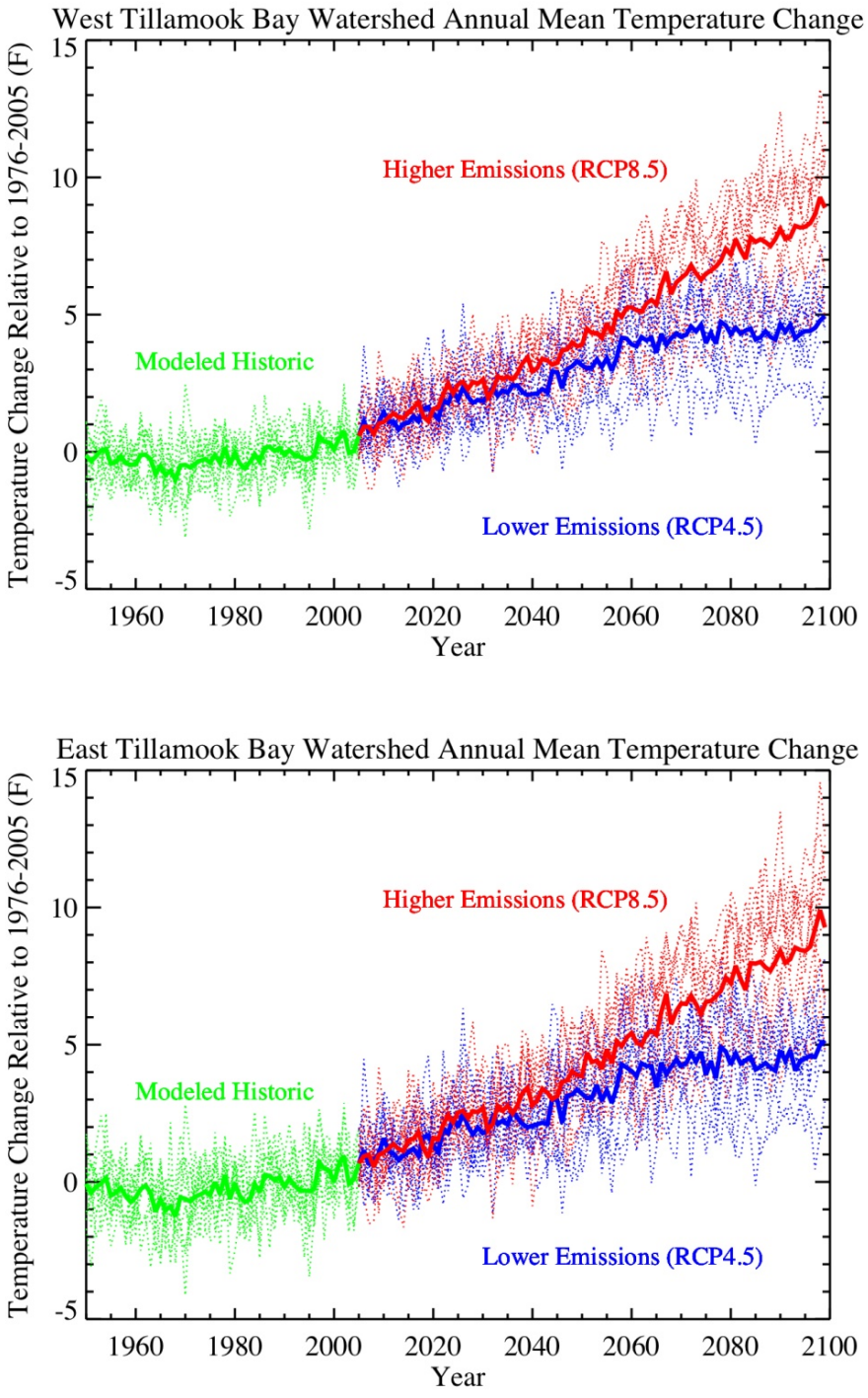

Figure 22: Annual mean temperature, modeled historical and projected. Each light dotted line is the output from one model. Heavy lines are the ensemble (group) mean. Change is relative to the 1976–2005 baseline.

Table 5 illustrates the projected changes from the 1976–2005 baseline in seasonal and annual mean temperatures for the three decadal periods in the 21st century. The greatest warming is projected to occur during the summer months. Again, it is only after mid-century that the amount of warming begins to differ substantially between the two RCPs.

East Domain Projected Change in Mean Temperature (F)

	2010–2039		2040–2069		2070–2099	
	RCP4.5	RCP8.5	RCP4.5	RCP8.5	RCP4.5	RCP8.5
Annual	1.7	2.0	3.2	4.3	4.3	7.3
Winter	1.7	2.0	3.1	4.0	4.1	6.9
Spring	1.6	1.7	2.9	3.7	3.8	6.2
Summer	1.8	2.3	3.7	5.1	4.9	8.5
Fall	1.6	1.9	3.1	4.5	4.2	7.7

West Domain Projected Change in Mean Temperature (F)

	2010–2039		2040–2069		2070–2099	
	RCP4.5	RCP8.5	RCP4.5	RCP8.5	RCP4.5	RCP8.5
Annual	1.7	2.0	3.2	4.3	4.2	7.2
Winter	1.7	2.0	3.1	4.0	4.1	6.7
Spring	1.6	1.8	2.8	3.7	3.7	6.1
Summer	1.8	2.3	3.7	5.0	4.8	8.3
Fall	1.6	1.9	3.1	4.5	4.2	7.6

Table 5: Projected temperature changes.

Extremes

Figures 23–26 illustrate projected changes in four metrics related to extreme temperature: the average number of days per year when the temperature equals or exceeds 90 °F; the average temperature of the hottest day of the year; the average number of days per year when the temperature equals or drops below 32 °F; and the average temperature of the coldest day of the year. For each figure the colored bars illustrate the "ensemble mean", i.e., the average of all the models. Each "x" illustrates the results for each individual model. The "spread" of individual model results gives an indication of the uncertainty of the projection.

Figures 23 and 24 illustrate projected changes in the number of days per year where the maximum temperature is greater than or equal to 90 °F and the average temperature of the hottest day of the year. Note that for the West domain, days greater than or equal to 90 °F are (and are projected to remain) rare, even under high emissions. A dramatic increase in the number of hot days is projected for the East domain, especially under high emissions.

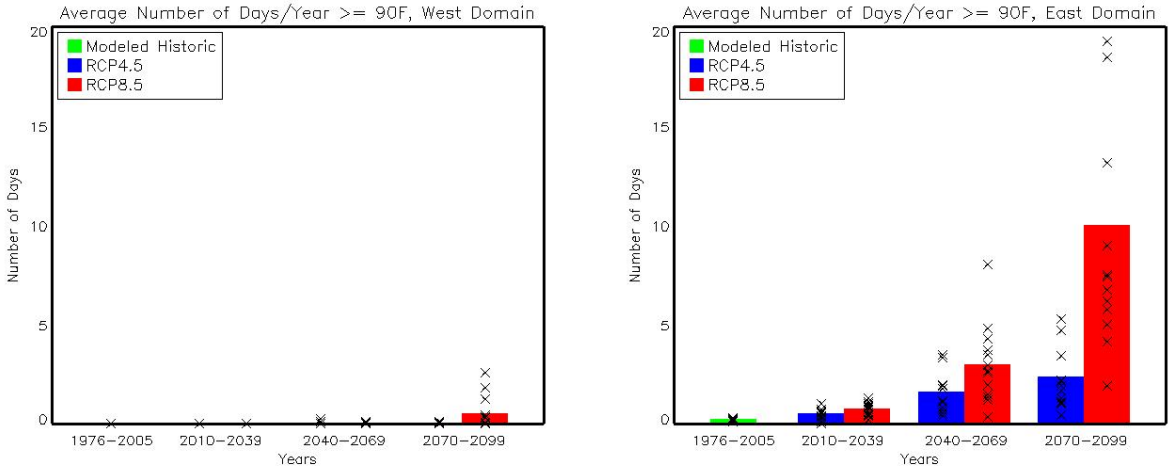

Figure 23: Number of days per year where the maximum temperature equals or exceeds 90F. Colored bars are the ensemble mean; each "x" represents an individual model result.

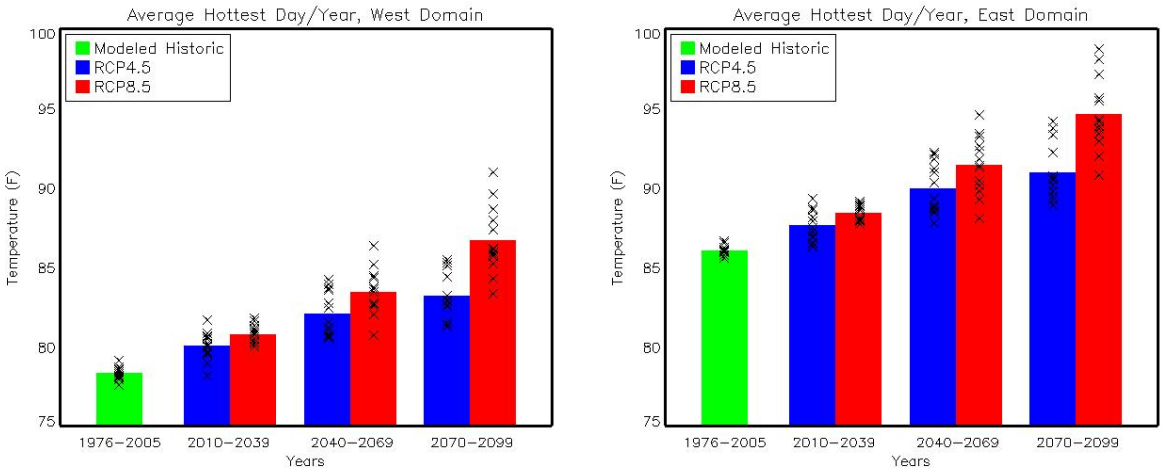

Figure 24: Average temperature of the hottest day of the year. Colored bars are the ensemble mean; each "x" represents an individual model result.

Figures 25 and 26 illustrate projected changes in the number of days per year where the minimum temperature is less than or equal to 32 °F; and the average temperature of the coldest day of the year. Both domains are projected to see a decrease in freezing days, with a dramatic decrease for the East domain under both emissions scenarios. The average temperature of the coldest day of the year rises markedly for both domains.

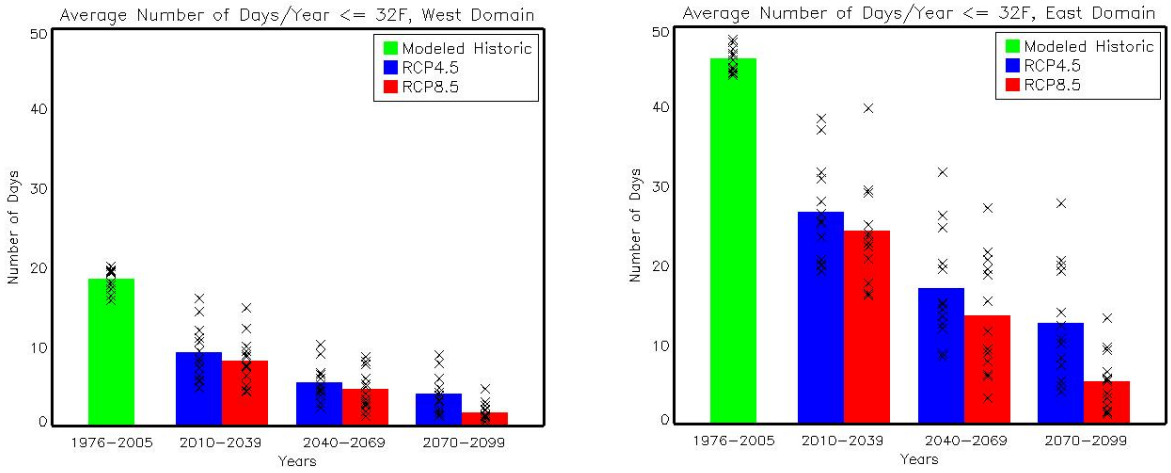

Figure 25: Average number of days per year where the minimum temperature equals or drops below 32 °F. Colored bars are the ensemble mean; each "x" represents an individual model result.

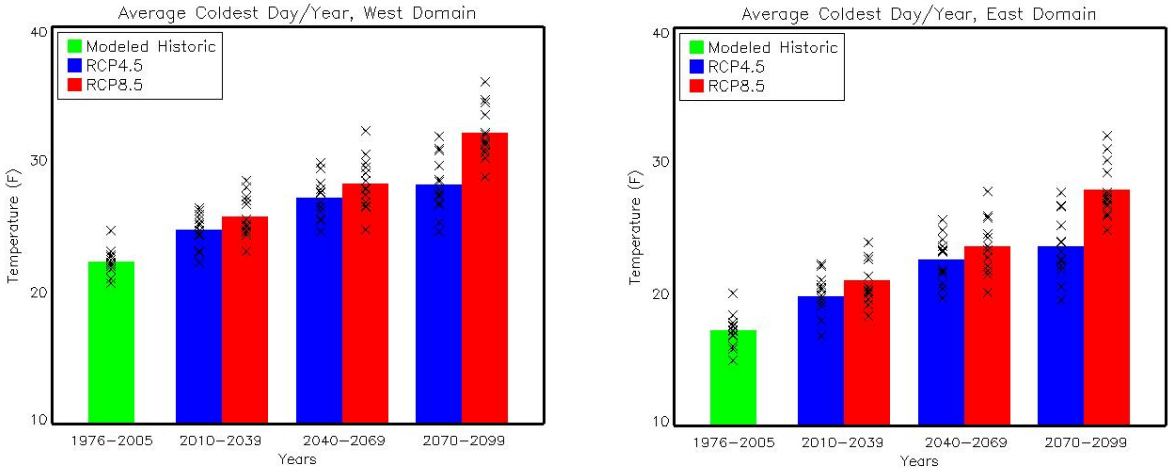

Figure 26: Average temperature of the coldest day of the year. Colored bars are the ensemble mean; each "x" represents an individual model result.

Precipitation Projections

Means

Figure 27 illustrates the annual mean precipitation for the TBW. The data suggests a slight (5%) increase in annual mean precipitation by the year 2100 (also see Table 6).

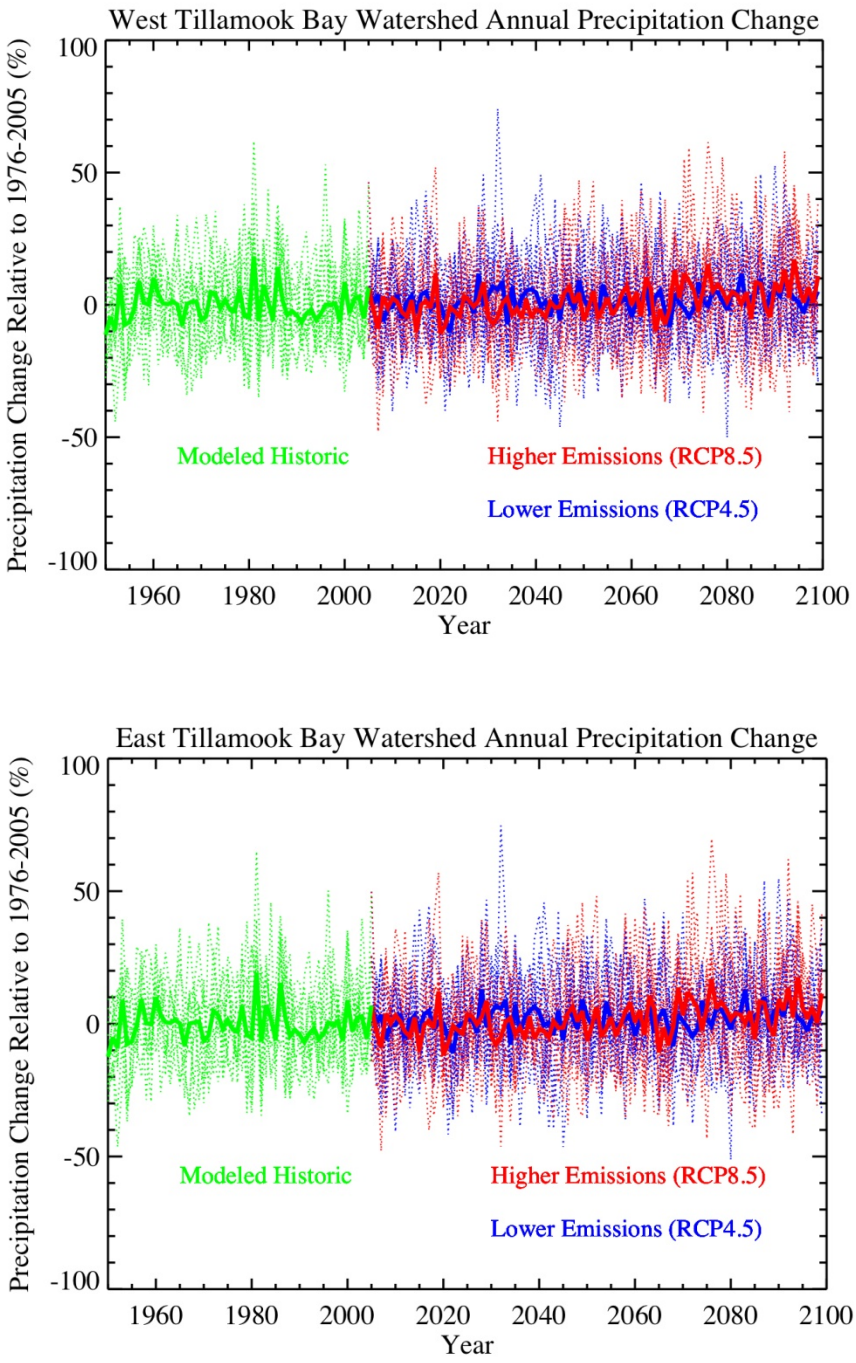

Figure 27: Annual mean precipitation, modeled historical and projected. Light lines are the output from one model. Heavy lines are the ensemble (group) mean. Percent change is compared to the 1976–2005 baseline.

Table 6 illustrates the projected changes from the 1976–2005 baseline in seasonal and annual mean precipitation for the three decadal periods in the 21st century. This data suggests a slight increase in the annual mean precipitation throughout the 21st century. However, there is a notable difference in seasonality, with the spring and summer projected to be drier, and the fall and winter wetter.

East Domain Projected Change in Precipitation (%)

	2010–2039		2040–2069		2070–2099	
	RCP4.5	RCP8.5	RCP4.5	RCP8.5	RCP4.5	RCP8.5
Annual	1	-1	2	1	3	5
Winter	2	2	6	5	7	13
Spring	-3	-5	-2	-4	-4	-3
Summer	-5	-11	-15	-21	-14	-19
Fall	3	-2	1	3	5	5

West Domain Projected Change in Precipitation (%)

	2010–2039		2040–2069		2070–2099	
	RCP4.5	RCP8.5	RCP4.5	RCP8.5	RCP4.5	RCP8.5
Annual	1	-1	2	1	3	5
Winter	3	2	6	5	7	13
Spring	-3	-5	-2	-3	-4	-3
Summer	-4	-10	-14	-20	-14	-19
Fall	3	-1	1	3	6	5

Table 6: Projected precipitation changes. Blue cells indicate an increase in precipitation; orange-brown cells indicate a decrease.

Extremes

Figures 28–30 illustrate projected changes in three metrics related to extreme precipitation: the number of days per year when 2 inches or more of precipitation falls ("wet days"); the average wettest day per year; and the number of months in drought conditions for a 30-year period. A drought month is defined as a month that receives less than 80% of the average precipitation for that month in the 1976–2005 baseline period. For each figure the colored bars illustrate the "ensemble mean", i.e., the average of all the models. Each "x" illustrates the results for each individual model. The "spread" of individual model results gives an indication of the uncertainty of the projection.

Figure 28 projects a slight increase in the number of wet days per year by the end of the century. In Figure 29 the amount of precipitation on the wettest day of the year is projected to increase a little as well by the end of the century (most notably under high emissions). The number of drought days in Figure 30 is not projected to change much.

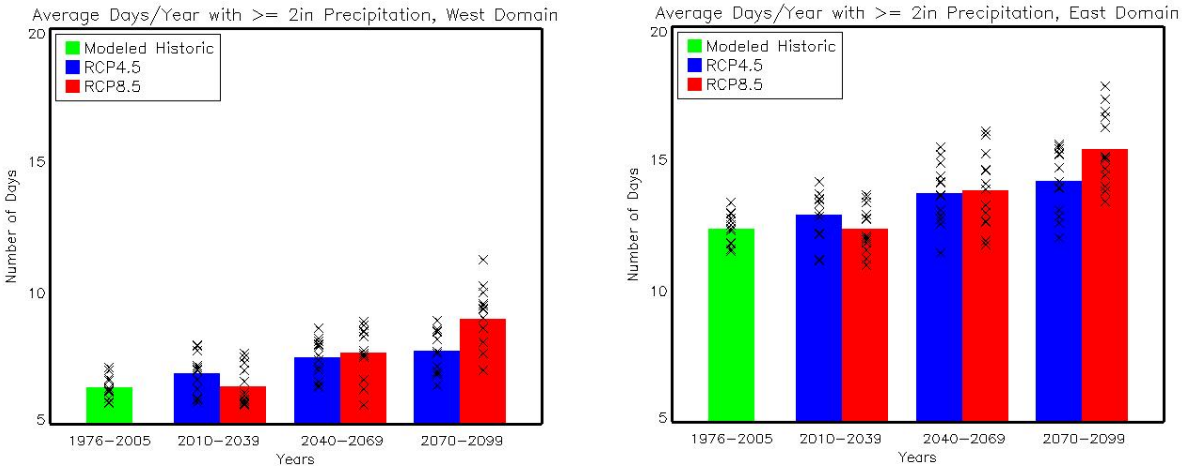

Figure 28: Average number of days per year receiving at least 2 inches of precipitation. Colored bars are the ensemble mean; each "x" represents an individual model result.

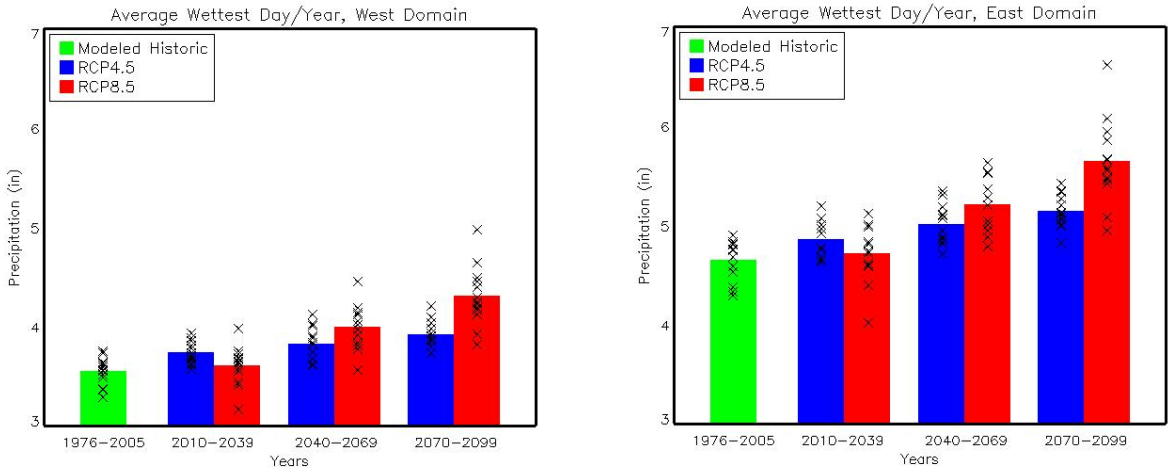

Figure 29: Average precipitation on the wettest day of the year. Colored bars are the ensemble mean; each "x" represents an individual model result.

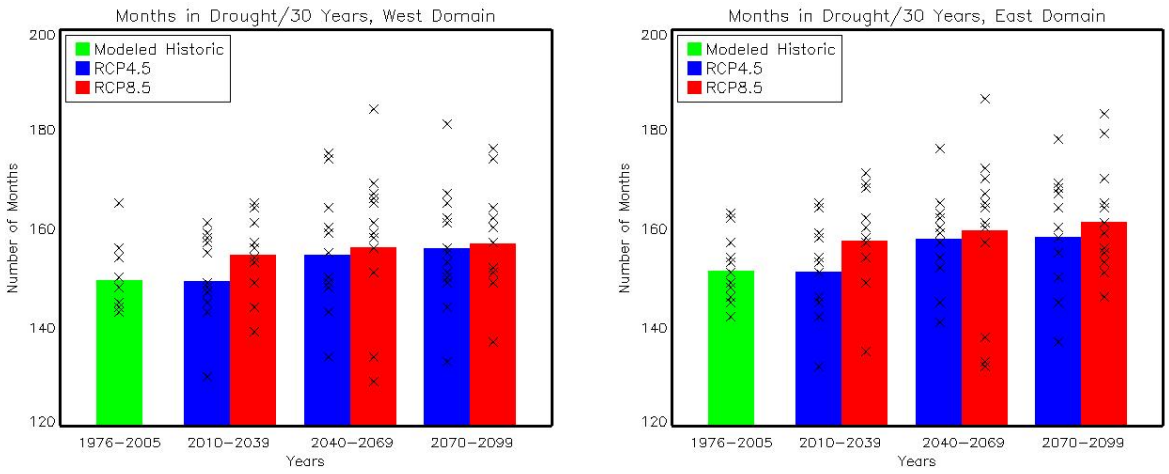

Figure 30: Number of months in drought (less than 80% of 30-year average precipitation). Colored bars are the ensemble mean; each "x" represents an individual model result.

Sea Level

A variety of sea level rise projections have been generated for the 21st century (and beyond). Recently, the National Research Council (NRC) generated its own set of projections for sea level rise along the US West Coast using the latest available science (NRC 2012). The NRC report also compared these projections to other projections. Figure 31 summarizes these global sea level rise findings for the years 2030, 2050, and 2100. For the projections used in Figure 31, Vermeer and Rahmstorf (2009) is a semi-empirical method based on the observed historical correlation between global temperature and sea level change; IPCC (2007) is the model-based projection from the IPCC's Fourth Assessment Report. These two sets of projections were chosen for comparison as they are representative of semi-empirical and model-based sea level rise projection methodologies (respectively).

While the NRC (2012) projection values for sea level rise in 2030 and 2050 are similar to Vermeer and Rahmstorf, they have a somewhat wider range. For 2100, the NRC committee projects a rise which is substantially higher than the IPCC (2007), but at the lower end of the Vermeer and Rahmstorf range.

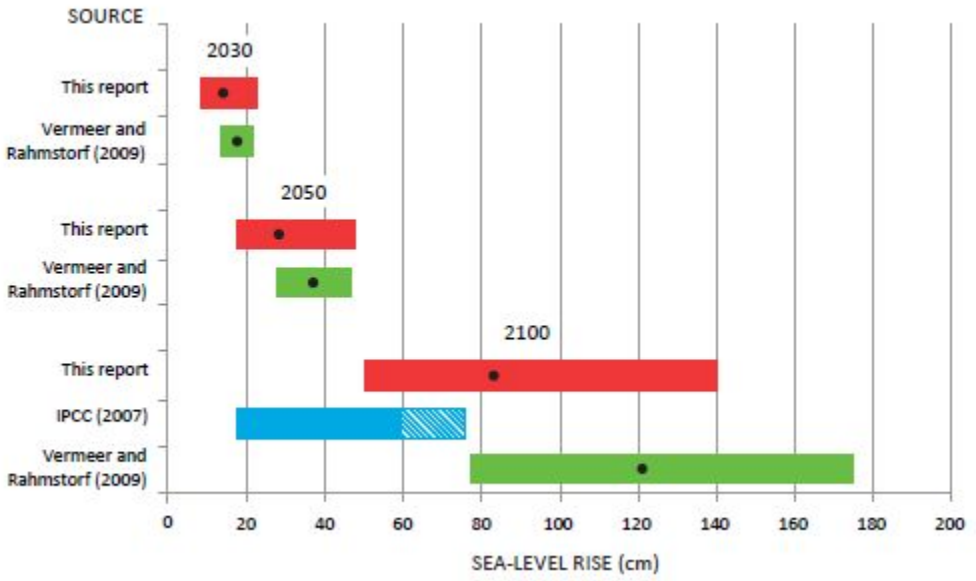

Figure 31: NRC global sea level rise projections, compared to Vermeer and Rahmstorf (semi-empirical) and IPCC (2007) model based projections. Black dots are the projection; colored bars indicate the projection range. For "IPCC (2007)" the hashed lines represent ice sheet discharge. Projections labeled "This report" refer to NRC 2012. 20.0 cm = 7.9 inches.

As mentioned earlier, sea levels along the US West Coast are impacted by global sea level rise, as well as several regional effects such as: ocean and atmospheric circulation patterns (e.g., the El Niño-Southern Oscillation and the Pacific Decadal Oscillation); the effects of land ice mass changes; groundwater withdrawal or recharge; and tectonics along the coast.

Table 7 presents projections for local sea level rise along the West Coast (NRC 2012). These projections include all the factors mentioned above (thermal expansion, melting ice, vertical land motion, etc.). Note how projections for areas north of Cape Mendocino (Seattle and Newport) are lower than for those south of that point (primarily due to the difference in vertical land motion). Figure 32 summarizes graphically the findings of NRC 2012 for regional (OR, WA, and CA) and global sea level rise as compared to the semi-empirical approach.

Regional Sea Level Rise Projections (cm) Relative to Year 2000						
	2030		2050		2100	
Location	Projection	Range	Projection	Range	Projection	Range
Seattle	6.6 ± 5.6	-3.7–22.5	16.6 ± 10.5	-2.5–47.8	61.8 ± 29.3	10.0–143.0
Newport	6.8 ±5.6	-3.5–22.7	17.2 ± 10.3	-2.1–48.1	63.3 ± 28.3	11.7–142.4
San Francisco	14.4 ± 5.0	4.3–29.7	28.0 ± 9.2	12.3–60.8	91.9 ± 25.5	42.4–166.4
Los Angeles	14.7 ± 5.0	4.6–30.0	28.4 ± 9.0	12.7–60.8	93.1 ± 24.9	44.2–166.5

Table 7: Sea level rise projections. Projection = mean ± std deviation for A1B emissions; Range = means for B1 (low) and A1F1 (high) emissions

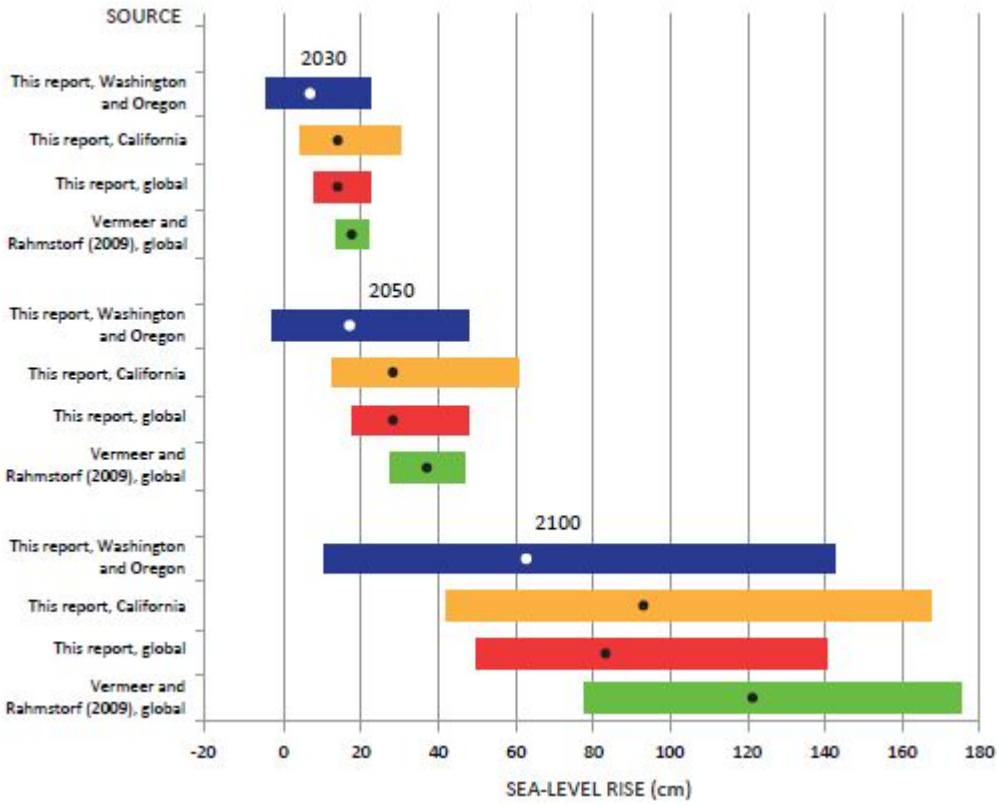

Figure 32: Global vs. regional projections for sea level rise, US West Coast. Black dots are the projection; colored bars indicate the projection range. "This report" refers to NRC (2012). 20.0 cm = 7.9 inches.

Figure 33 shows the additional inundation expected at high tide for a representative amount of sea level rise (2 ft/61 cm). This screen shot is from an interactive National Oceanic and Atmospheric Administration (NOAA) website available at http://www.csc.noaa.gov/digitalcoast/tools/slrviewer/. This website allows a user to specify an amount of sea level rise (0–6 ft) and explore how this may affect tide inundation levels above current Mean Higher High Water (MHHW). NOAA notes that the website is useful as a screening level tool for use in identifying areas of concern and should not be used in an attempt to predict exactly where floods will occur.

Figure 33: Projected inundation east of Garibaldi, OR assuming 2 ft/61 cm of sea level rise. Dark blue area represents current MWWH level at high tide. Light blue shading indicates additional inundation due to sea level rise.

Ocean Acidification

The ultimate effect of ocean acidification on calcifiers is still an active research topic. Ocean acidification is an important consideration for the Tillamook estuary, due to projections for a marked increase in acidification along the entire Oregon coast. By 2050 the nearshore 6.2 mile/10 km domain may see an annual mean pH as low as 7.82 ± 0.04 (compared to a pre-industrial value of 8.03 ± 0.03) (Gruber et al. 2012).

Virtually every major biological function of marine organisms has been shown to respond to acidification changes in seawater, including photosynthesis, respiration rate, growth rates, calcification rates, reproduction, and recruitment. Much of the attention has focused on carbonate-based animals and plants which form the foundation of our marine ecosystems. An increase in ocean acidity has been shown to impact shell-forming marine organisms from plankton to benthic mollusks, echinoderms, and corals (Barton et al. 2012; Doney et al. 2009). Many calcifying species exhibit reduced calcification and growth rates in laboratory experiments under high-CO_2 conditions. For example, in the Netarts estuary in Oregon, it was demonstrated that increased acidification negatively impacted oyster production, due to decreased vigor in later life stages (Barton et al. 2012). Ocean acidification also causes an increase in carbon fixation rates in some photosynthetic organisms (both calcifying and noncalcifying) (Doney et al. 2009; Feely et al. 2012; Ocean Carbon and Biogeochemistry Program 2008; Smith and Baker 2008).

Conclusion

Climate change is an issue with global, as well as local, ramifications. Due to unique local conditions, the local climate may change more (or less) than the average global climate. It is important to understand these local variations so that local adaptation efforts can be most effective.

The northwestern coast of Oregon is already experiencing changes due to climate change in the form of increasing average, maximum, and minimum temperatures. While trends in average precipitation have not been apparent, the data suggests an increase in extreme precipitation events. As for the marine environment, regional sea level has risen in most (but not all) locations, while increased acidity has been measured in the coastal waters near the Tillamook Bay.

Changes are projected to continue into the future. Temperatures will continue to increase, with projections suggesting a dramatic increase in hot (at least 90 °F) days in the eastern part of the TBW, especially under a high emissions scenario. Annual precipitation may increase only slightly, but projections call for an accentuation of the seasonal cycle (especially drier summers and springs). All indications are that the sea level will continue to rise. While positive vertical land motion somewhat minimizes the effect of global sea level rise along the Oregon coast, it does not completely neutralize it. The oceans are projected to become even more acidic as the concentration of atmospheric CO_2 increases, with unpredictable results.

Given the inevitability of at least some climate change in the future, it is important to evaluate systems for their sensitivity to these changes. In addition, adaptations that enhance system resilience to climate change should be considered.

List of Works Cited

Abatzoglou J.T., and T.J. Brown (2011) A comparison of statistical downscaling methods suited for wildfire applications, *International Journal of Climatology* 32, 5, 772–780, doi: 10.1002/joc.2312

Bader, D.C., C. Covey, W.J. Gutowski Jr., I.M. Held, K.E. Kunkel, R.L. Miller, R.T. Tokmakian, and M.H. Zhang (2008) Climate Models: An Assessment of Strengths and Limitations, A Report by the U.S. Climate Change Science Program and the Subcommittee on Global Change Research, Department of Energy, Office of Biological and Environmental Research, Washington, D.C.

Barnola, J.-M., D. Raynaud, C. Lorius, and N.I. Barkov (2003) Historical CO_2 record from the Vostok ice core, In Trends: A Compendium of Data on Global Change, Carbon Dioxide Information Analysis Center, Oak Ridge National Laboratory, U.S. Department of Energy, Oak Ridge, TN, USA

Barton, A., B. Hales, G. G. Waldbusser, C. Langdon, R. A. Feely, The Pacific oyster, Crassostrea gigas, shows negative correlation to naturally elevated carbon dioxide levels: Implications for near-term ocean acidification effects, Limnology and Oceanography 57 (3), 698–710 (2012), doi:10.4319/lo.2012.57.3.0698

Bindoff, N.L., J. Willebrand, V. Artale, A, Cazenave, J. Gregory, S. Gulev, K. Hanawa, C. Le Quéré, S. Levitus, Y. Nojiri, C.K. Shum, L.D. Talley and A. Unnikrishnan (2007) Observations: Oceanic Climate Change and Sea Level. In: Climate Change 2007: The Physical Science Basis. Contribution of Working Group I to the Fourth Assessment Report of the Intergovernmental Panel on Climate Change [Solomon, S., D. Qin, M. Manning, Z. Chen, M. Marquis, K.B. Averyt, M. Tignor and H.L. Miller (eds.)]. Cambridge University Press, Cambridge, United Kingdom and New York, NY, USA.

Caldeira, K., and M.E. Wickett (2005) Ocean model predictions of chemistry changes from carbon dioxide emissions to the atmosphere and ocean, *Journal of Geophysical Research: Oceans* 110, C09S04,doi: 10.1029/2004JC002671

Church, J.A., N.J. White, L.F. Konikow, C.M. Domingues, J.G. Cogley, E. Rignot, J.M., Gregory, M.R. van den Broeke, A.J. Monaghan, and I. Velicogna (2011) Revisiting the earth's sea level and energy budgets from 1961 to 2008, *Geophysical Research Letters* 38, L18601, doi: 10.1029/2011GL048794

CMIP 2012, http://cmip-pcmdi.llnl.gov/cmip5/

Doney, S.C., V.J. Fabry, and R.A. Feely (2009) Ocean Acidification: The Other CO_2 Problem, *Annual Review of Marine Science* 1, 169–192, doi: 10.1146/annurev.marine.010908.163834

Etheridge, D.M., L.P. Steele, R.L. Langenfelds, R.J. Francey, J.-M.Barnola, and V.I. Morgan (1998) Historical CO_2 records from the Law Dome DE08, DE08-2, and DSS ice cores, In Trends: A Compendium of Data on Global Change, Carbon Dioxide Information Analysis Center, Oak Ridge National Laboratory, U.S. Department of Energy, Oak Ridge, TN, USA

Feely, R.A., C.L. Sabine, K. Lee, W. Berelson, J. Kleypas, V.J. Fabry, and F.J. Millero (2004) Impact of Anthropogenic CO_2 on the $CaCO_3$ System in the Oceans, *Science* 305, 362–366, doi: 10.1126/science.1097329

Feely, R.A., V.J. Fabry, and J.M. Guinotte (2008) Ocean acidification of the North Pacific Ocean, PICES Press, 1, 16, 22–26

Feely, R.A., C.L. Sabine, R.H. Byrne, F.J. Millero, A.G. Dickson, R. Wanninkhof, A. Murata, L.A. Miller, and D. Greeley (2012) Decadal changes in the aragonite and calcite saturation state of the Pacific Ocean, *Global Biogeochemical Cycles* 26, GB3001, doi: 10.1029/2011GB004157

Forster, P., V. Ramaswamy, P. Artaxo, T. Berntsen, R. Betts, D.W. Fahey, J. Haywood, J. Lean, D.C. Lowe, G. Myhre, J. Nganga, R. Prinn, G. Raga, M. Schulz and R. Van Dorland (2007), Changes in Atmospheric Constituents and in Radiative Forcing, In: Climate Change 2007: The Physical Science Basis, Contribution of Working Group I to the Fourth Assessment Report of the Intergovernmental Panel on Climate Change [Solomon, S., D. Qin, M. Manning, Z. Chen, M. Marquis, K.B. Averyt, M.Tignor and H.L. Miller (eds.)], Cambridge University Press, Cambridge, United Kingdom and New York, NY, USA

Gruber, N., C. Hauri, Z. Lachkar, D. Loher, T. L. Frölicher, G-K. Plattner (2012) Rapid Progression of Ocean Acidification in the California Current System, *Science* 337, 220–223, doi: 10.1126/science.1216773

Hansen, J., R. Ruedy, M. Sato, and K. Lo (2010) Global surface temperature change, *Reviews of Geophysics* 48, RG4004, doi: 10.1029/2010RG000345

Hauri, C., N. Gruber, G.-K.Plattner, S. Alin, R.A. Feely, B. Hales, and P.A. Wheeler (2009) Ocean acidification in the California Current System, *Oceanography* 22, 4, 60–71, doi: 10.5670/oceanog.2009.97

Hawkins, E., and R. Sutton (2009) The potential to narrow uncertainty in regional climate predictions, *Bulletin of the American Meteorological Society* 90, 1095–1107, doi: 10.1175/2009BAMS2607.1

IPCC (2007) Summary for Policymakers, In: Climate Change 2007: The Physical Science Basis, Contribution of Working Group I to the Fourth Assessment Report of the Intergovernmental Panel on Climate Change [Solomon, S., D. Qin, M. Manning, Z. Chen, M. Marquis, K.B. Averyt, M.Tignor and H.L. Miller (eds.)], Cambridge University Press, Cambridge, United Kingdom and New York, NY, USA

Jouzel, J., V. Masson-Delmotte, O. Cattani, G. Dreyfus, S. Falourd, G. Hoffmann, B. Minster, J. Nouet, J.-M. Barnola, J.A. Chappellaz, H. Fischer, J.C. Gallet, S.J. Johnsen, M. Leuenberger, L. Loulergue, D. Luethi, H. Oerter, F. Parrenin, G. Raisbeck, D. Raynaud, A. Schilt, J. Schwander, E. Selmo, R. Souchez, R. Spahni, B. Stauffer, J.P. Steffensen, B. Stenni, T.F. Stocker, J.-L.Tison, M. Werner, and E.W. Wolff (2007) Orbital and millennial Antarctic climate variability over the past 800,000 years, *Science* 317, 5839, 793–797, doi: 10.1126/science.1141038

Kiehl, J.T., and K.E. Trenberth (1997) Earth's Annual Global Mean Energy Budget, *Bulletin of the American Meteorological Society* 78, 197–208, doi: 10.1175/1520-0477

Komar, P.D., J.C. Allan, and P. Ruggiero (2011) Sea level Variations along the U.S. Pacific Northwest Coast: Tectonic and Climate Controls, *Journal of Coastal Research* 27, 5, 808–823, doi: 10.2112/JCOASTRES-D-10-00116.1

Kunkel, K.E., M.A. Palecki, L. Ensor, K.G. Hubbard, D.A. Robinson, K.T. Redmond, and D.R. Easterling, (2009) Trends in twentieth-century U.S. snowfall using a quality-controlled dataset, *Journal of Atmospheric and Oceanic Technology* 26, 33–44

Lüthi, D., M. Le Floch, B. Bereiter, T. Blunier, J.-M.Barnola, U. Siegenthaler, D. Raynaud, J. Jouzel, H. Fischer, K. Kawamura, and T.F. Stocker (2008) High-resolution carbon dioxide concentration record 650,000 – 800,000 years before present, *Natur e*453, 379–382, doi: 10.1038/nature06949

Manning, M.R., J. Edmonds, S. Emori, A. Grubler, K. Hibbard, F. Joos, M. Kainuma, R.F. Keeling, T. Kram, A.C. Manning, M. Meinshausen, R. Moss, N. Nakicenovic, K. Riahi, S.K. Rose, S. Smith, R. Swart, and D.P. van

Vuuren (2010) Misrepresentation of the IPCC CO_2 emission scenarios, *Nature Geoscience* 3, 376–377, doi: 10.1038/ngeo880

Menne, M.J., C.N. Williams, Jr., and R.S. Vose (2012) United States Historical Climatology Network (USHCN) Version 2 Serial Monthly Dataset, Carbon Dioxide Information Analysis Center, Oak Ridge National Laboratory, Oak Ridge, TN, USA

Mote, P.W., and E.P. Salathé (2010) Future Climate in the Pacific Northwest, *Climatic Change* 102, 29–50, doi: 10.1007/s10584-010-9848-z

Neftel, A., H. Friedli, E. Moor, H. Lötscher, H. Oeschger, U. Siegenthaler, and B. Stauffer (1994) Historical CO_2 record from the Siple Station ice core, In Trends: A Compendium of Data on Global Change, Carbon Dioxide Information Analysis Center, Oak Ridge National Laboratory, U.S. Department of Energy, Oak Ridge, TN, USA

National Research Council (NRC) Committee on Sea Level Rise in California, Oregon, and Washington (2012) Sea Level Rise for the Coasts of California, Oregon, and Washington: Past, Present, and Future, www.nap.edu/catalog.php?record_id=13389

NOAA NCDC, http://www.ncdc.noaa.gov/cmb-faq/anomalies.php

NOAA SL, http://tidesandcurrents.noaa.gov/sltrends/sltrends.html

OCAR, Oregon Climate Assessment Report (2010), www.occri.net/ocar

Ocean Carbon and Biogeochemistry Program, Subcommittee on Ocean Acidification (December 2, 2008) Ocean Acidification- Recommended Strategy for a U.S. National Research Program

Orr, J.C., V.J. Fabry, O. Aumont, L. Bopp, S.C. Doney, R.A. Feely, A. Gnanadesikan, N. Gruber, A. Ishida, F. Joos, R.M. Key, K. Lindsay, E. Maier-Reimer, R. Matear, P. Monfray, A. Mouchet, R.G. Najjar, G.-K. Plattner, K.B. Rodgers, C.L. Sabine, J.L. Sarmiento, R. Schlitzer, R.D. Slater, I.J. Totterdell, M.-F. Weirig, Y. Yamanaka, and A. Yool(2005) Anthropogenic ocean acidification over the twenty-first century and its impact on calcifying organisms, *Nature* 437, 681–686, doi: 10.1038/nature04095

Petit, J.-R., J. Jouzel, D. Raynaud, N.I. Barkov, J.-M.Barnola, I. Basile, M.L. Bender, J.A. Chappellaz, J.C. Davis, G. Delaygue, M. Delmotte, V. Kotlyakov, M.R. Legrand, V.Y. Lipenkov, C. Lorius, L. Pepin, C. Ritz, E.S. Saltzman, and M. Stiévenard (1999) Climate and atmospheric history of the past 420,000 years from the Vostok ice core, Antarctica, *Nature* 399, 6735, 429–436, doi: 10.1038/20859

Roe, G.H., and K.C. Armour (2011) How sensitive is climate sensitivity?,*Geophysical Research Letters* 38, L14708, doi: 10.1029/2011GL047913

Roe, G.H., and M.B. Baker (2007) Why Is Climate Sensitivity So Unpredictable? ,*Science* 318, 629–632, doi: 10.1126/science.1144735

Ruggiero, P., P.D. Komar, and J.C. Allan (2010) Increasing wave heights and extreme-value projections: The wave climate of the U.S. Pacific Northwest, *Coastal Engineering* 57, 539–552

Sabine, C.L., R.A. Feely, N. Gruber, R.M. Key, K. Lee, J.L. Bullister, R. Wanninkhof, C.S. Wong, D.W.R. Wallace, B. Tilbrook, F.J. Millero, T.-H. Peng, A. Kozyr, T. Ono,and A.F. Rios (2004) The Oceanic Sink for Anthropogenic CO_2, *Science* 305, 367–371

Sabine, C.L., and R.A. Feely in Greenhouse Gas Sinks, D. Reay, N. Hewitt, J. Grace, K. Smith, Eds. (CABI, Oxfordshire, UK, 2007)

Santer, B.D., C. Mears, F.J. Wentz, K.E. Taylor, P.J. Gleckler, T.M.L. Wigley, T.P. Barnete, J.S. Boyle, W. Bruggemann, N.P. Gillett, S.A. Klein, G.A. Meehl, T. Nozawa, D.W. Pierce, P.A. Stott, W.M. Washington, and M.F. Wehner (2007) Identification of human-induced changes in atmospheric moisture content, *Proceedings of the National Academy of Science* 104, n39, 15248–15253, doi: 10.1073/pnas.0702872104

Siegenthaler, U., T.F. Stocker, E. Monnin, D. Lüthi, J. Schwander, B. Stauffer, D. Raynaud, J.-M. Barnola, H. Fischer, V. Masson-Delmotte, and J. Jouzel (2005) Stable carbon cycle - Climate relationship during the Late Pleistocene, *Science* 310, 5752, 1313–1317, doi: 10.1126/science.1120130

Shakun, J.D., P.U. Clark, F. He, S.A. Marcott, A.C. Mix, Z. Liu, B. Otto-Bliesner, A. Schmittner, and E. Bard (2012) Global warming preceded by increasing carbon dioxide concentrations during the last deglaciation, *Nature* 484, 49–54, doi: 10.1038/nature10915

Smith, E., and J. Baker (2008) Pacific Island Ecosystem Complex, from Osgood, K.E. (editor), Climate Impacts on U.S. Living Marine Resources: National Marine Fisheries Service Concerns, Activities and Needs, U.S. Dep. Commerce, NOAA Technical Memorandum, NMFS-F/SPO-89, 118 p

Solomon, S., D. Qin, M. Manning, R.B. Alley, T. Berntsen, N.L. Bindoff, Z. Chen, A. Chidthaisong, J.M. Gregory, G.C. Hegerl, M. Heimann, B. Hewitson, B.J. Hoskins, F. Joos, J. Jouzel, V. Kattsov, U. Lohmann, T. Matsuno, M. Molina, N. Nicholls, J. Overpeck, G. Raga, V. Ramaswamy, J. Ren, M. Rusticucci, R. Somerville, T.F. Stocker, P. Whetton, R.A. Wood, and D. Wratt (2007) Technical Summary, In: Climate Change 2007: The Physical Science Basis. Contribution of Working Group I to the Fourth Assessment Report of the Intergovernmental Panel on Climate Change [Solomon, S., D. Qin, M. Manning, Z. Chen, M. Marquis, K.B. Averyt, M. Tignor and H.L. Miller (eds.)], Cambridge University Press, Cambridge, United Kingdom and New York, NY, USA

Tillamook Bay Environmental Characterization: A Scientific and Technical Summary (1998) Tillamook Bay National Estuary Project

Trenberth, K.E., P.D. Jones, P. Ambenje, R. Bojariu, D. Easterling, A. Klein Tank, D. Parker, F. Rahimzadeh, J.A. Renwick, M. Rusticucci, B. Soden and P. Zhai (2007) Observations: Surface and Atmospheric Climate Change. In: Climate Change 2007: The Physical Science Basis. Contribution of Working Group I to the Fourth Assessment Report of the Intergovernmental Panel on Climate Change [Solomon, S., D. Qin, M. Manning, Z. Chen, M. Marquis, K.B. Averyt, M. Tignor and H.L. Miller (eds.)]. Cambridge University Press, Cambridge, United Kingdom and New York, NY, USA

vanVuuren, D., J. Edmonds, M. Kainuma, K. Riahi, A. Thomson, K. Hibbard, G. Hurtt, T. Kram, V. Krey, J.-F. Lamarque, T. Masui, M. Meinshausen, N. Nakicenovic, S. Smith, and S. Rose (2011) The representative concentration pathways: an overview,*Climatic Change* 109, 5–31, doi: 10.1007/s10584-011-0148-z